



MASTER THESIS

Dynamical properties of few bosons trapped in an harmonic potential

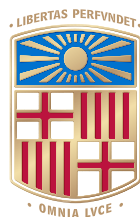
Author:

David LEDESMA MORAGA

Supervisors:

Dr. Artur POLLS MARTÍ

Dr. Bruno JULIÁ-DÍAZ



UNIVERSITAT DE
BARCELONA

Dep. Física Quàntica i Astrofísica
Facultat de Física
Universitat de Barcelona

September 8, 2018

Acknowledgements

I would like to sincerely thank my advisors, Dr. Artur Polls and Dr. Bruno Juliá-Díaz, specially for their constant help and support during the project, and particularly their patience. I would like also to thank them for providing me all their knowledge and giving me the possibility of assisting to very special meetings.

I also would like to thank my family and friends for their companion and enlivenment during this project and my life.

Contents

Acknowledgements	iii
1 Introduction	1
2 Homogeneous system	3
2.1 Non-interacting limit and mean-field	3
2.2 Tonks-Girardeau limit and Fermi-Bose mapping	4
3 1D system trapped in an H.O. potential	9
3.1 Hamiltonian of the system	9
3.2 Virial Theorem	9
3.3 Non-interacting and Tonks-Girardeau limits	11
3.4 Gross Pitaevskii and Thomas Fermi approaches	12
4 Two particles trapped in a 1D H.O. potential	17
4.1 Separation of the center of mass	17
4.2 First order perturbation theory	18
4.3 Solution of the relative Hamiltonian: exact diagonalization	18
4.4 Convergence of the method	19
4.5 Energy spectrum	20
4.6 Contributions to the total energy	22
5 Breathing mode	25
5.1 Dynamic Structure Function (DSF): Excitation operator	25
5.2 Calculations for $N=2$	26
5.3 Results for two particles	28
5.4 Excitation of the C.M.	30
6 Sum Rules	33
6.1 The energy sum rules	33
6.2 Derivation of the sum rules	34
6.2.1 M_{-1} sum rule	34
6.2.2 M_1 sum rule	35
6.2.3 M_3 sum rule	37
6.3 Non-interacting and Tonks-Girardeau limits	38
7 Sum Rules applied to a 2 bosons system	41
7.1 Behaviour of the sum rules and contribution of the C.M. peak	41
7.2 Excitation energy and reentrant behaviour	43

Chapter 1

Introduction

Quantum few-body problems appear in many branches of physics, ranging from nuclear and high energy physics, to ultra-cold atomic gases and condensed matter physics. Notorious examples are for instance the study of small nuclei [1], like the triton, the study of hadrons as compounds of constituents quarks [2], the trapped few-atom problem which can be prepared in ultra-cold atomic labs [3]-[6] or few-electron quantum dots in condensed matter [7]. In all cases, there are some common features and techniques which can be applied to many of the systems despite the very different energy and size scales involved in the problem. All these few-body systems can exhibit different kind of phases, depending on the interaction among the constituents, e.g. long or short ranged, spin dependent, etc., which give rise to different quantum mechanical properties. Among the latter, the onset of quantum mechanical correlations among the constituents, requiring beyond mean-field approaches in the description, are particularly interesting nowadays.

In this work we will concentrate on systems of ultra-cold atoms trapped in external potentials. Whenever possible, e.g. non-interacting, we will explore many-body properties of the system to then concentrate on a more detailed study of the few-body case. Recent experiments have shown a great improvement in control of the experimental parameters of the Bose-Einstein condensates (BEC), such as their geometry, the number of particles condensed and the interactions induced in the system. Nowadays, it is possible to generate a BEC confined to one dimension just by increasing substantially the transversal frequencies of the optical lattices which sustain the condensate [8]. It has also been reported the possibility of precisely controlling the interaction among particles by means of a magnetically induced Feshbach resonances [9]. Thus open us a new way to understand how many-body quantum mechanical correlations build in few-body systems [3]-[6] & [10]-[13], as in these systems, the clash between a strong interaction and the confinement to a low-dimensional geometry ends in a magnification of the quantum effects, inducing important quantum correlations in the system.

These new experimental procedures provide us a theoretical many-body laboratory that permits to either corroborate or discard some mean-field theories developed in the last century, which are thought to be good approaches for weak-interacting systems. Another interesting example to study this interplay between confinement and interaction, is the Tonks-Girardeau gas, which basically consists

on having atoms with a very strong repulsive interaction confined to a one dimensional geometry. Taking advantage of these new experimental methods, it is possible to study the evolution of the static and dynamical properties of this kind of systems from the non-interacting to the strongly interacting regimes.

The minimal example of the Tonks-Girardeau system is that of two particles trapped in a harmonic oscillator potential [14]. Such system offers an appropriate playground to study this interplay between quantum many-body correlations and statistics. For the case of a contact interaction potential, two noteworthy limits are well known. This kind of contact interaction potentials are realistic in the case of ultra-cold atomic systems [15], and even have also been used in effective interaction theories in nuclear physics [16]. In the particular case of two particles, in absence of interactions the two atoms populate the lowest energy single particle state, producing the minimal version of a Bose-Einstein condensed state, whereas in the infinite interaction limit the two bosons resemble in many ways two spin-less non-interacting fermions, producing the so called Tonks-Girardeau (TG) limit [17].

This thesis is organized in the following way. First, in chapter 2 we introduce the homogeneous system, which is most simple system of this kind only containing a δ -contact interaction. Next, in chapter 3 we describe the N particles one dimensional Tonks-Girardeau system with a confinement given by an harmonic potential, whereas in chapter 4 we do analyze more extensively the same system but only for 2 particles. In the following chapter, the breathing mode (excitation) of this system is explained; and in chapter 6 the general energy sum rules of the dynamic structure function associated to a given excitation operator are derived. After that, in chapter 7, these sum rules are applied to the two particle system. Finally, in chapter 8 we summarize the whole project and draw the conclusions.

Chapter 2

Homogeneous system

We start by considering the homogeneous system, characterized by a linear density $n = N/L$ where N is the number of bosons enclosed in a linear box of length L . To simulate the homogeneous system, we implement periodic boundary conditions and take the thermodynamic limit with $N \rightarrow \infty$ and $L \rightarrow \infty$ keeping the ratio n constant. We concentrate our efforts on the Lieb-Liniger model ([18]), which takes a δ -contact interaction to describe the inter-atomic interactions which has been used frequently in the literature.

The Hamiltonian for this system has two terms : the kinetic energy and the interaction energy.

$$\mathcal{H} = -\frac{\hbar^2}{2m} \sum_i^N \frac{d^2}{dx_i^2} + g \sum_{i<j}^N \delta(x_i - x_j), \quad (2.1)$$

where g is a parameter which characterizes the strength of the δ -contact interaction. In this work we consider only the repulsive case with $g \geq 0$.

2.1 Non-interacting limit and mean-field

In the non-interacting limit, the system would simply consists on having N free bosons of mass m enclosed in a linear box of length L with periodic boundary conditions. The system could be described as a product state of N free-particles properly symmetrized.

The use of periodic boundary conditions allows us to consider the plane wave single-particle basis.

$$\psi_0(x_1, x_2, \dots, x_N) = \hat{S} \left(\prod_{i=1}^N \phi_k(x_i) \right), \quad (2.2)$$

where the operator \hat{S} is the responsible for the symmetrization of the wave function. The single particle wave functions are defined as :

$$\phi_k(x_i) = \frac{1}{\sqrt{L}} e^{ip_k x_i}, \quad p_k = \frac{2\pi n_k}{L}, \quad (2.3)$$

and where n_k can be any integer.

In the ground state the system is fully condensed with all the particles in the zero momentum state which is allowed by the periodic boundary conditions. In this case, the product of the single-particle wave functions with $k = 0$, i.e. , $\psi_0(x_1, x_2, \dots, x_N) = (\prod_{i=1}^N \phi_0(x_i))$, is already symmetric.

In this regime, using perturbation theory, we can derive the energy per particle as the expectation value of the interaction energy in the ground state of the free system

$$e = \frac{E}{N} = \frac{V}{N} = \frac{1}{2}ng, \quad (2.4)$$

and the chemical potential

$$\mu = \frac{dE}{dN} = ng. \quad (2.5)$$

Notice, that both are linear with the density number and the interaction strength. In the non-interacting limit we will not observe any kind of two-body correlations, obtaining a constant two-body distribution of $g(x) = 1$.

2.2 Tonks-Girardeau limit and Fermi-Bose mapping

In the Tonks-Girardeau limit we assume an infinite interaction strength g , so that the particles in our system become impenetrable point-like bosons. In this limit we can apply the Fermi-Bose mapping ([17],[20]), which in essence consists on transforming a fermionic wave-function (ψ_F) into a bosonic one (ψ_B). The most general expression for this mapping is given by

$$\psi_B(x_1, \dots, x_N, t) = A(x_1, \dots, x_N)\psi_F(x_1, \dots, x_N, t), \quad (2.6)$$

where A is a unit antisymmetric function

$$A(x_1, \dots, x_N) \equiv \prod_{i>j}^N \text{sgn}(x_i - x_j), \quad (2.7)$$

in which

$$\text{sgn}(x) \equiv \frac{x}{|x|}. \quad (2.8)$$

By construction, the new wave-function ψ_B is symmetric under any permutation. In the case of the the ground state of the system, the expression reduces to

$$\psi_0^B(x_1, \dots, x_N) = |\psi_0^F(x_1, \dots, x_N)|, \quad (2.9)$$

where $\psi_0^F(x_1, \dots, x_N)$ is the ground state of a free-fermion system, which is symmetrized by applying the absolute value on the Slater determinant of the underlying free Fermi sea.

This mapping allows us to obtain the ground state of the system as the absolute value of the Slater determinant of the lowest N single-particle plane waves

$$\psi_0(1, \dots, N) = \frac{1}{\sqrt{N!}} \left| \det \left(\frac{1}{\sqrt{L}} e^{ip_j x_l} \right) \right|. \quad (2.10)$$

The highest occupy level defines an effective Fermi momentum, which is related to the linear density through

$$N = \frac{L}{2\pi} \int_{-k_F}^{k_F} dk \Rightarrow n = \frac{k_F}{\pi}. \quad (2.11)$$

While the energy and chemical potential are given by

$$E = \frac{L}{2\pi} \int_{-k_F}^{k_F} \frac{\hbar^2 k^2}{2m} dk \Rightarrow e = \frac{E}{N} = \frac{\pi^2 \hbar^2}{6m} n^2 \quad (2.12)$$

$$\mu = \frac{dE}{dN} = \frac{\pi^2 \hbar^2}{2m} n^2. \quad (2.13)$$

In this strongly interacting limit emerge important two-body correlations which affect the two-body distribution function:

$$g(x_{12}) = \frac{N(N-1)}{n^2} \int \psi^*(1, \dots, N) \psi(1, \dots, N) dx_2 \dots dx_N, \quad (2.14)$$

which essentially gives the probability to find two particles at a given distance x_{12} and coincides with the two-body distribution function of the underlying one-dimensional free Fermi sea. 2.1

$$g(x) = 1 - \frac{\sin^2(n\pi x)}{(n\pi x)^2}. \quad (2.15)$$

The two-body distribution function is zero for $x_{12} = 0$, i.e., two particles can not be at the same point if the strength of the interaction goes to infinity. Then the distribution function heals to 1, with small oscillations that never bring $g(x_{12})$ above 1.

This two-body distribution fulfills the sequential condition

$$n \int_{-\infty}^{\infty} (g(x) - 1) dx = -1. \quad (2.16)$$

Directly related to $g(x)$ we have the static structure function defined as

$$S(k) = 1 + n \int e^{ikx} (g(x) - 1) dx. \quad (2.17)$$

This is the Fourier transform of the two-body distribution function, which is shown in Fig. 2.2. The static structure function contains useful physical information. For

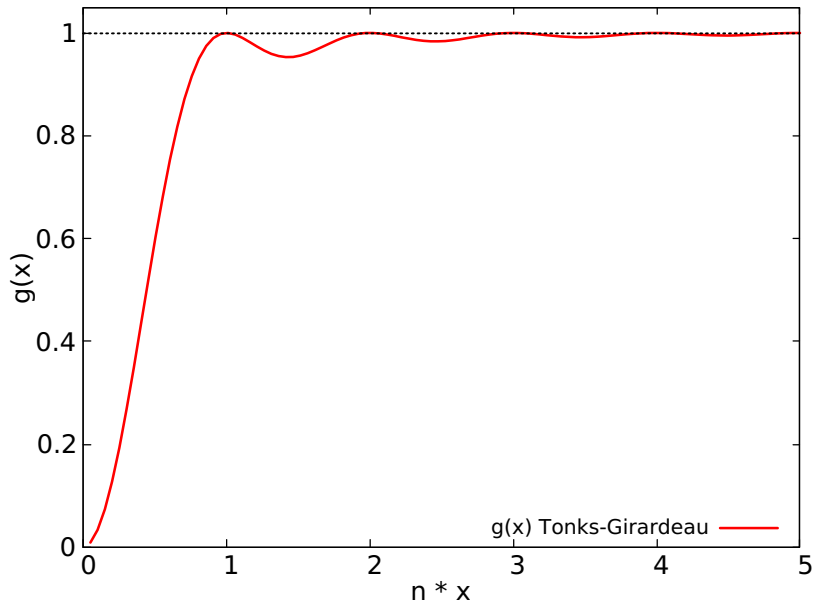


FIGURE 2.1: Two-body distribution function for an homogeneous boson system, with a delta contact interaction in the Tonks-Girardeau limit ($g \rightarrow \infty$). It departs from 0 at the origin, since the particles in this regime are impenetrable and point-like. Notice that is the same as for a free Fermi gas at $T=0$.

instance the slope of $S(k)$ when $k \rightarrow 0$ is related to the speed of sound in the system,

$$S(k) \rightarrow \frac{\hbar k}{2mc_s} \Rightarrow c_s = \frac{\hbar \pi n}{m}, \quad (2.18)$$

which is in agreement with the thermodynamic estimation of the speed of sound calculated from the derivative of the chemical potential:

$$mc_s^2 = n \frac{d\mu}{dn} \Rightarrow \frac{\hbar \pi n}{m}, \quad (2.19)$$

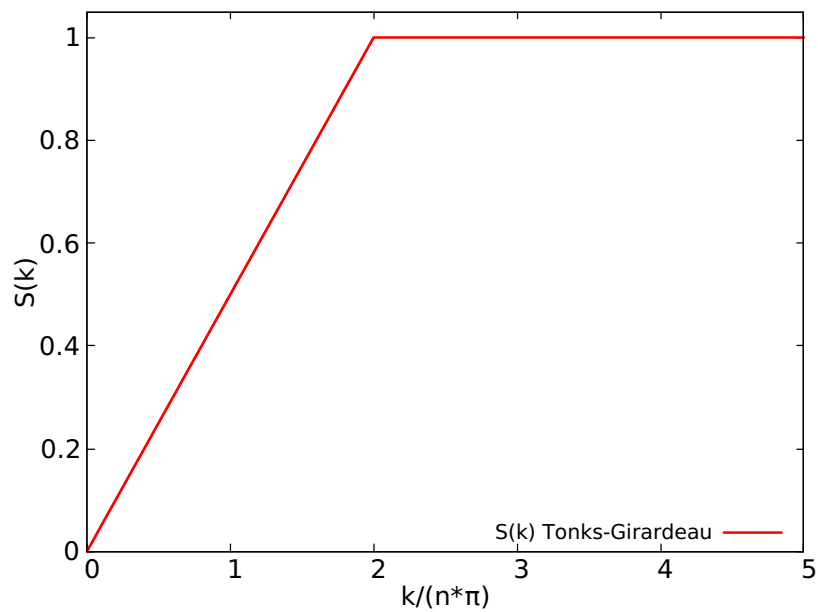


FIGURE 2.2: Static distribution function for an homogeneous boson system, with a delta contact interaction in the Tonks-Girardeau limit ($g \rightarrow \infty$). It departs from 0 at the origin, and end up in a limit value $S(k) \rightarrow 1$ for $\frac{k}{n\pi} \geq 2$. since the particles in this regime are impenetrable and point-like. Notice that is the same as for a free Fermi gas at $T=0$ and that also fulfills the sequential condition.

Chapter 3

1D system trapped in an H.O. potential

In this chapter we introduce a one dimensional bosonic N -particles system confined in an harmonic oscillator potential. The interactions between the particles are described by a δ -contact interaction with strength g . First we analyze two extreme limits: the mean field or weakly interacting regime which includes the non-interacting case, with $g = 0$, and the strongly interacting regime, also known as the Tonks-Girardeau limit, when $g \rightarrow \infty$. In the TG regime the quantum correlations dominate the behavior and as a consequence the mean field, which is not able to incorporate particle-particle correlations to the wave function, gives a very poor description of the system. As mentioned in the introduction, these systems with different number of particles and a good control of the tuning of the strength of the interaction have been experimentally realized ([3, 5, 13, 21, 22]).

3.1 Hamiltonian of the system

The Hamiltonian for many identical bosons trapped in a one dimensional harmonic oscillator and interacting through a contact potential can be read as,

$$\mathcal{H} = -\frac{\hbar^2}{2m} \sum_i \frac{d^2}{dx_i^2} + \sum_i \frac{1}{2} m \omega x_i^2 + g \sum_{i < j} \delta(x_i - x_j), \quad (3.1)$$

where the inter-atomic interaction is described by a Dirac delta function with strength g . In order to simplify the notation, from now on, we will work in H.O. units. In this case, the Hamiltonian is written as:

$$\mathcal{H} = -\frac{1}{2} \sum_i \frac{d^2}{dx_i^2} + \frac{1}{2} \sum_i x_i^2 + g \sum_{i < j} \delta(x_i - x_j). \quad (3.2)$$

3.2 Virial Theorem

Note that the Hamiltonian in 3.2 is formally the same for fermionic and bosonic systems. It is useful to decompose the Hamiltonian in three contributions: the kinetic energy (T), the energy associated to the harmonic potential (V_{HO}) which plays the role of a confining potential and the interaction energy (V_{int}). Therefore we have

$H = T + V_{HO} + V_{int}$ with

$$T = \sum_{i=1}^N -\frac{1}{2} \frac{d^2}{dx_i^2}, V_{HO} = \sum_{i=1}^N \frac{x_i^2}{2}, V_{int} = \sum_{i<j}^N g\delta(x_i - x_j). \quad (3.3)$$

When the system is composed by bosons, one can compute analytically the energy in two limiting cases: 1) the non-interacting case and, 2) the extremely repulsive case. But in this section we want to concentrate on the virial theorem which allows to establish a relation between the different energy contributions. The virial theorem is based on the scaling transformation of the many-body wave-function and how the expectation values of the different pieces of the Hamiltonian transform under these scaling transformations. To this end, we first define a new wave function through the scaling transformation,

$$\Psi_\lambda(x_1, x_2, \dots, x_n) = \lambda^{N/2} \Psi(\lambda x_1, \lambda x_2, \dots, \lambda x_n). \quad (3.4)$$

The new wave-function ψ_λ has exactly the same normalization than ψ , since

$$\begin{aligned} \langle \psi_\lambda | \psi_\lambda \rangle &= \int dx_1 dx_2 \dots dx_N \psi_\lambda(x_1, x_2, \dots, x_n)^* \psi_\lambda(x_1, x_2, \dots, x_n) \\ &= \lambda^N \int dx_1 dx_2 \dots dx_N \psi(\lambda x_1, \lambda x_2, \dots, \lambda x_n)^* \psi(\lambda x_1, \lambda x_2, \dots, \lambda x_n) \\ &= \lambda^N \int \frac{1}{\lambda^N} dy_1 dy_2 \dots dy_N \psi(y_1, y_2, \dots, y_n)^* \psi(y_1, y_2, \dots, y_n) = \langle \psi | \psi \rangle, \end{aligned} \quad (3.5)$$

where we have implemented the change of variable $y_i = \lambda x_i$. The harmonic oscillator energy is transformed as

$$\begin{aligned} V_{HO}(\lambda) &= \langle \psi_\lambda | \sum_{i=1}^N \frac{x_i^2}{2} | \psi_\lambda \rangle \\ &= \frac{N}{2} \lambda^N \int dx_1 dx_2 \dots dx_N \psi(\lambda x_1, \lambda x_2, \dots, \lambda x_n)^* x_1^2 \psi(\lambda x_1, \lambda x_2, \dots, \lambda x_n) \\ &= \frac{N}{2} \lambda^N \int \frac{1}{\lambda^N} dy_1 \dots dy_N \psi(y_1, \dots, y_N)^* \frac{y_1^2}{\lambda^2} \psi(y_1, \dots, y_N) \\ &= \frac{1}{\lambda^2} \langle \psi | V_{HO} | \psi \rangle = \frac{1}{\lambda^2} V_{HO}(\lambda = 1). \end{aligned} \quad (3.6)$$

The transformation of the interaction energy reads:

$$\begin{aligned} V_{int}(\lambda) &= \langle \psi_\lambda | \sum_{i<j} g\delta(x_i - x_j) | \psi \rangle \\ &= \frac{N(N-1)}{2} g \lambda^N \int dx_1 \dots dx_N \psi(\lambda x_1, \lambda x_2, \dots, \lambda x_N) \delta(x_1 - x_2) \psi(\lambda x_1, \lambda x_2, \dots, \lambda x_N) \\ &= \frac{N(N-1)}{2} g \lambda^N \int \frac{1}{\lambda^N} dy_1 \dots dy_N \psi(y_1, y_2, \dots, y_N) \lambda \delta(y_1 - y_2) \psi(y_1, y_2, \dots, y_N) \\ &= \lambda \langle \psi | V_{int} | \psi \rangle = \lambda V_{int}(\lambda = 1), \end{aligned} \quad (3.7)$$

and for the kinetic energy we have

$$\begin{aligned}
T(\lambda) &= \langle \psi_\lambda | \sum_{i=1}^N -\frac{1}{2} \frac{d^2}{dx_i^2} | \psi_\lambda \rangle = -\frac{N}{2} \lambda^N \int dx_1 \dots dx_N \psi(\lambda x_1, \dots, \lambda x_N)^* \frac{d}{dx_1^2} \psi(\lambda x_1, \dots, \lambda x_N) \\
&= -\frac{N}{2} \lambda^N \int \frac{1}{\lambda^N} dy_1 \dots dy_N \psi(y_1, \dots, y_N)^* \lambda^2 \frac{d^2}{dy_1^2} \psi(y_1, \dots, y_N) \\
&= \lambda^2 T(\lambda = 1).
\end{aligned} \tag{3.8}$$

After all these transformation, the final effect of the scaling can be written as

$$E_\lambda = \langle \psi_\lambda | H | \psi_\lambda \rangle = \lambda^2 T(\lambda = 1) + \frac{1}{\lambda^2} V_{HO}(\lambda = 1) + \lambda V_{int}(\lambda = 1). \tag{3.9}$$

Now we know that at $\lambda = 1$, the energy function E_λ has a stationary point, i.e.

$$\left. \frac{dE_\lambda}{d\lambda} \right|_{\lambda=1} = 0, \tag{3.10}$$

since $\psi(x_1, \dots, x_N)$ is taken to be an eigenfunction, which in particular could be the ground state. Therefore,

$$\left. \frac{dE_\lambda}{d\lambda} \right|_{\lambda=1} = 2\lambda T(\lambda = 1) - \frac{2}{\lambda^3} V_{HO}(\lambda = 1) + V_{int}(\lambda = 1), \tag{3.11}$$

and imposing the stationary condition, we reach

$$\left. \frac{dE_\lambda}{d\lambda} \right|_{\lambda=1} = 0 = 2T(\lambda = 1) - 2V_{HO}(\lambda = 1) + V_{int}(\lambda = 1), \tag{3.12}$$

which is valid for any eigenstate of the system. Also notice that the virial relation is valid for both type of particles; for bosons and for fermions.

3.3 Non-interacting and Tonks-Girardeau limits

It is easy to figure out how the non-interacting limit behaves: as we have no interaction, we just deal with a system composed by particles confined by an harmonic oscillator. Therefore, the Hamiltonian of the system reduces to

$$\mathcal{H} = -\frac{1}{2} \sum_i \frac{d^2}{dx_i^2} + \frac{1}{2} \sum_i x_i^2, \tag{3.13}$$

and the total energy of the system will be the sum of the single-particle states of one dimensional harmonic oscillator. Knowing that the eigenvalues of a one dimensional H.O. are $E_n^{HO} = n + 1/2$ (in H.O. units), the ground state energy of the system is

$$E_0 = \sum_i^N E_0^{HO} = \frac{N}{2}, \tag{3.14}$$

having all the particles in the single-particle state $n = 0$ of the H.O. Therefore, the wave-function for the ground state of the system is given by

$$\psi_0(x_1, x_2, \dots, x_N) = \prod_{i=1}^N \phi_0(x_i), \quad (3.15)$$

where $\phi_0(x_i) = \left(\frac{1}{\pi}\right)^{1/4} e^{-x_i^2/2}$ is the ground state of the single-particle harmonic oscillator.

In the Tonks-Girardeau limit, $g \rightarrow \infty$ we rely again on the Fermi-Bose mapping to calculate the energy of the ground-state of the system. As has been explained in previous sections, in this case, the ground state is the absolute value of the Slater determinant built as if the particles were fermions. In the case of N particles they occupy the first N lowest single-particle energy levels of the harmonic oscillator potential, therefore

$$E_0 = \left(\frac{1}{2} + \frac{3}{2} + \dots + \frac{2N-1}{2} \right) = \frac{N^2}{2}. \quad (3.16)$$

Notice that the absolute value of the Slater determinant guarantees the symmetric character of the wave function under the exchange of particles, which is a necessary condition to describe identical bosons. It is also worth to mention the different behavior of the total energy on the number of particles in these two limits: in the non-interacting case is just linear in the number of particles while becomes quadratic a function in the strongly interacting case.

3.4 Gross Pitaevskii and Thomas Fermi approaches

In the mean field approach we assume a trial wave function for our system such as

$$\psi(x_1, x_2, \dots, x_N) = \prod_{i=1}^N \phi(x_i), \quad (3.17)$$

with all the particles in the same single-particle state. The expectation value of the Hamiltonian in this wave function is given by

$$\langle \psi | H | \psi \rangle = N \langle \phi | -\frac{1}{2} \frac{d^2}{dx^2} + \frac{1}{2} x^2 | \phi \rangle + g \frac{N(N-1)}{2} \langle \phi(x_1) \phi(x_2) | \delta(x_1 - x_2) | \phi(x_1) \phi(x_2) \rangle, \quad (3.18)$$

where the two-body matrix element $\langle \phi(x_1) \phi(x_2) | g \delta(x_1 - x_2) | \phi(x_1) \phi(x_2) \rangle = g \int dx |\phi(x)|^4$. To find the optimal (less energy) wave function of that type, we perform a functional variation of the previous energy functional, which is complemented with the introduction of a Lagrange multiplier μ to impose that the variations in the wave function respect the normalization condition. The Lagrange multiplier has the meaning of the chemical potential of the system

$$\frac{\delta}{\delta \phi^*} [\langle \psi | H | \psi \rangle - \mu \langle \psi | \psi \rangle] = 0, \quad (3.19)$$

from which we get a non-linear differential Hartree-Bose equation for ϕ , usually known as the Gross-Pitaevskii equation

$$-\frac{1}{2} \frac{d^2}{dx^2} \phi(x) + \frac{1}{2} x^2 \phi(x) + (N-1)g |\phi(x)|^2 \phi(x) = \mu \phi(x), \quad (3.20)$$

where $\phi(x)$ is normalized to unity.

It is important to remark that the virial relation is also valid in the mean-field approximation

$$2t - 2v_{HO} + v_{int} = 0, \quad (3.21)$$

where

$$t = \langle \phi | -\frac{1}{2} \frac{d^2}{dx^2} | \phi \rangle, \quad v_{HO} = \langle \phi | \frac{1}{2} x^2 | \phi \rangle, \quad v_{int} = g \frac{N-1}{2} \langle \phi(x_1) \phi(x_2) | \delta(x_1 - x_2) | \phi(x_1) \phi(x_2) \rangle \quad (3.22)$$

being ϕ the solution to the Gross-Pitaevskii equation.

A useful approximation to the Gross-Pitaevskii equation which is known as the Thomas-Fermi approach, which is valid when the kinetic energy contribution can be neglected in front of both potentials energies; the interaction and the harmonic oscillator ones. Then the Gross-Pitaevskii equation reduces to

$$\frac{1}{2} x^2 + (N-1)g |\phi(x)|^2 = \mu. \quad (3.23)$$

From this equation we are able to isolate $|\phi(x)|^2$, and impose that the density should be always positive. From that assumption we obtain

$$\phi(x) = \begin{cases} \frac{1}{\sqrt{g(N-1)}} \sqrt{\mu - \frac{1}{2} x^2}, & -\sqrt{2\mu} < x < \sqrt{2\mu} \\ 0, & |x| > \sqrt{2\mu}. \end{cases} \quad (3.24)$$

To determine the value of μ , we impose the normalization of the wave function $\phi(x)$, so that

$$\frac{1}{g(N-1)} \int_{-\sqrt{2\mu}}^{\sqrt{2\mu}} \left[\mu - \frac{1}{2} x^2 \right] dx = 1. \quad (3.25)$$

Performing the integral we obtain one equation in terms of the chemical potential of the system

$$\int_{-\sqrt{2\mu}}^{\sqrt{2\mu}} \left[\mu - \frac{1}{2} x^2 \right] dx = 2 \int_0^{\sqrt{2\mu}} \left[\mu - \frac{1}{2} x^2 \right] dx = \frac{2^{5/2} \mu^{3/2}}{3}. \quad (3.26)$$

Then, imposing the normalization condition explained above, we obtain the chemical potential

$$\frac{1}{g(N-1)} \frac{2^{5/2} \mu^{3/2}}{3} = 1 \Rightarrow \mu = \left(\frac{(3g(N-1))^2}{2^5} \right)^{1/3}. \quad (3.27)$$

Once the chemical potential is known the wave function is fully determined and the total energy can be calculated assuming always that the kinetic energy is zero. We can start by the interaction energy per particle

$$\begin{aligned} v_{int} &= g \frac{N-1}{2} \langle \phi(x_1) \phi(x_2) | \delta(x_1 - x_2) | \phi(x_1) \phi(x_2) \rangle = g \frac{N-1}{2} \int_{-\sqrt{2\mu}}^{\sqrt{2\mu}} |\phi(x)|^4 dx \\ &= \frac{(N-1)}{g^2(N-1)^2} g \int_0^{\sqrt{2\mu}} \left[\mu^2 - \mu x^2 + \frac{1}{4} x^4 \right] dx \\ &= \frac{1}{g(N-1)} \left[\mu^2 x - \mu \frac{x^3}{3} + \frac{1}{5} x^5 \right]_0^{\sqrt{2\mu}} \\ &= \frac{1}{g(N-1)} \left(2^{1/2} - \frac{2^{3/2}}{3} + \frac{2^{5/2}}{5} \right) \mu^{5/2} = \frac{1}{5} \left(\frac{3g(N-1)}{2} \right)^{2/3}. \end{aligned} \quad (3.28)$$

and also compute the harmonic oscillator potential energy per particle

$$\begin{aligned} v_{HO} &= \langle \phi_{TF} | \frac{1}{2} x^2 | \phi_{TF} \rangle = \frac{1}{2} \int_{-\sqrt{2\mu}}^{\sqrt{2\mu}} \phi(x)^2 x^2 dx = \frac{1}{g(N-1)} \int_0^{\sqrt{2\mu}} \left[\mu - \frac{1}{2} x^2 \right] x^2 dx \\ &= \frac{1}{g(N-1)} \left[\mu \frac{x^3}{3} - \frac{1}{2} \frac{x^5}{5} \right]_0^{\sqrt{2\mu}} = \frac{1}{g(N-1)} \frac{2^{5/2}}{15} \mu^{5/2} \\ &= \frac{1}{10} \left[\frac{3g(N-1)}{2} \right]^{2/3} \end{aligned} \quad (3.29)$$

By adding both v_{HO} and v_{int} , the total energy per particle reads

$$e = \frac{1}{10} \left[\frac{3g(N-1)}{2} \right]^{2/3} + \frac{1}{5} \left(\frac{3g(N-1)}{2} \right)^{2/3} = \frac{3}{10} \left(\frac{3g(N-1)}{2} \right)^{2/3}. \quad (3.30)$$

This expression for the energy coincides with the one obtaining by integrating respect to N , the chemical potential as a function of the number of particles:

$$\mu \sim \frac{(3gN)^{2/3}}{2^{5/3}}, \quad (3.31)$$

and

$$E = \int_0^N \mu(N) dN = \int_0^N \frac{(3g)^{2/3}}{2^{5/3}} N^{2/3} dN = N \frac{3}{10} \left(\frac{3gN}{2} \right)^{2/3}, \quad (3.32)$$

which coincide with the previous expression when $N \approx (N-1)$ (i.e. for $N \gg 1$). Notice also that the virial theorem is still fulfilled in the TF approach. Since $t \equiv 0$,

$$2t - 2v_{HO} + v_{int} = 0 \Rightarrow v_{int}(N) = 2v_{HO}(N), \quad (3.33)$$

expression which we can clearly see that is fulfilled since

$$v_{int}^{TF} = \frac{1}{5} \left(\frac{3g(N-1)}{2} \right)^{2/3} = 2v_{HO}^{TF}. \quad (3.34)$$

In general, mean-field theories derived above describe properly the behaviour of our system when the interaction is weak and no correlations are present in the system. We have been able to describe the two extreme limits, interacting and strongly interacting, for any number of particles. It is very interesting, to see how the transition between the two regimes takes place, and the emergence of the quantum correlations that made useless the mean-field approach. Unfortunately, to solve the problem for intermediate g and any number of particles is numerically difficult. However, in the next chapter we will present the first steps towards a general solution by considering the simple case with $N = 2$.

Chapter 4

Two particles trapped in a 1D H.O. potential

Recent experiments with few ultra-cold atoms are able to probe the statistical properties of bosons and fermions in the smallest possible settings. Impressively, there are nowadays experiments with as few as just two fermions [3]-[6] or two bosons [13]. In the first case, the authors were able to produce the smallest version of the Fermi sea, populating it atom by atom. In the second, they managed to observe effects stemming from bosonic statistics with just two bosons.

Thus, in this chapter we will consider the minimal setting of just two bosons trapped in a harmonic oscillator potential. We will be able to study the transition from the non-interacting to the strongly interacting systems, thus going from the two-particle analog of a condensed system to the corresponding to the TG limit.

4.1 Separation of the center of mass

The Hamiltonian can be splitted into two parts: the first one corresponding to the center of mass of the system (C.M.), and the second one describing the relative motion. To this end, we define

$$\begin{aligned}\mu &\equiv m/2 \\ M &\equiv 2m \\ x_r &\equiv x_1 - x_2 \\ X &\equiv \frac{x_1 + x_2}{2},\end{aligned}\tag{4.1}$$

where μ is the reduced mass, M is the total mass of the system, X is the center of mass coordinate, and x_r is the relative coordinate. With these new variables, the Hamiltonian is splitted in two pieces $\mathcal{H} = \mathcal{H}_{CM} + \mathcal{H}_r$ with

$$\mathcal{H}_{CM} = -\frac{\hbar^2}{2M} \frac{d^2}{dX^2} + \frac{1}{2}M\omega^2 X^2\tag{4.2}$$

$$\mathcal{H}_r = -\frac{\hbar^2}{2\mu} \frac{d^2}{dx_r^2} + \frac{1}{2}\mu\omega^2 x_r^2 + g\delta(x_r).\tag{4.3}$$

The frequencies associated to both Hamiltonians are the same. However, the oscillator lengths are different. Now, it is convenient to express the Hamiltonians in the oscillator units of the original one:

$$\mathcal{H}_{CM} = -\frac{1}{4} \frac{d^2}{dX^2} + X^2 \quad (4.4)$$

$$\mathcal{H}_r = -\frac{d^2}{dx_r^2} + \frac{1}{4}x_r^2 + g\delta(x_r). \quad (4.5)$$

\mathcal{H}_{CM} is a harmonic oscillator Hamiltonian which is easy to solve. The problem reduces to the solution of \mathcal{H}_r .

4.2 First order perturbation theory

In order to get a first idea of the dependence of the energy of the system with the strength of the interaction, we can perform a first order perturbation calculation, which should provide a reasonable result for small interacting strengths. We assume that the relative Hamiltonian is given by

$$\mathcal{H}_r = \underbrace{-\frac{d^2}{dx_r^2} + \frac{1}{4}x_r^2}_{\text{unperturbed}} + \underbrace{g\delta(x_r)}_{\text{perturbation}} \equiv H_0 + gV_{\text{pert}}. \quad (4.6)$$

Then, using the analytical solution of the relative H.O., we obtain a spectrum at first order perturbation which is slightly shifted

$$E_r = E_{r,n}^{(0)} + g \langle \psi_{r,n}^{(0)} | \delta(x_r) | \psi_{r,n}^{(0)} \rangle = \left(n + \frac{1}{2} \right) + g |\psi_{r,n}^{(0)}(0)|^2, \quad (4.7)$$

Notice that only the states with non zero value of the wave function are affected by the interaction. For the specific case of the ground state we have:

$$E_{int} = g \langle \psi_{r,0}^{(0)} | \delta(x_r) | \psi_{r,0}^{(0)} \rangle = g \left(\frac{1}{2\pi} \right)^{1/2}, \quad (4.8)$$

and consequently, it provides a perturbed energy for the ground state of relative motion $E_r^0 = 1/2 + g \left(\frac{1}{2\pi} \right)^{1/2}$.

4.3 Solution of the relative Hamiltonian: exact diagonalization

As \mathcal{H}_{CM} and \mathcal{H}_r commute, the wave functions associated to the C.M. and relative motion factorize, so we can solve each one separated

$$\Psi(X, x_r) = \phi(X)\psi(x_r). \quad (4.9)$$

The \mathcal{H}_{CM} is an harmonic oscillator Hamiltonian with the spectrum $E_k^{CM} = (k + 1/2)$ where k are the number of quanta associated to the center of mass motion. The wave-functions associated to the C.M. are given by

$$\Psi_k = \left(\frac{a}{\pi}\right)^{1/4} \frac{1}{\sqrt{2^k k!}} H_k(\sqrt{a}X) e^{-aX^2/2}, \quad (4.10)$$

where H_k are the Hermite's polynomials and $a \equiv M\omega/\hbar$. Notice that $a_{cm} = 2$, whereas $a_r = \frac{1}{2}$ in the H.O. units.

To diagonalize the relative part we will use the following procedure. We choose a finite number of non-interacting energy eigenstates of the harmonic oscillator, $\{\psi_0(x_r), \psi_2(x_r), \dots, \psi_{2M}(x_r)\}$ corresponding to $\mathcal{H}_r^{(0)}$ (here $M + 1$ will be the total number of modes we want to use). Notice that in order to fulfill the requirements of the bosonic symmetry, we consider only the modes associated to even functions. The matrix elements of H_r are

$$\begin{aligned} \langle \Psi_m | H_r | \Psi_n \rangle &= \left(n + \frac{1}{2}\right) \delta_{m,n} + g \int dx_r \Psi_n(x_r) \Psi_m(x_r) \delta(x_r) \\ &= \left(n + \frac{1}{2}\right) \delta_{m,n} + g \Psi_n(0) \Psi_m(0), \end{aligned} \quad (4.11)$$

where $\Psi_i(0)$ are the H.O. wave functions at the origin.

Diagonalizing the truncated Hamiltonian we get approximate solutions, whose eigenvalues are upper bounds of the corresponding exact solutions.

$$H_r \bar{\Psi}_l = \bar{E}_l^{(r)} \bar{\Psi}_l. \quad (4.12)$$

4.4 Convergence of the method

In practice we use a huge number of modes, M up to 1500, to guarantee the convergence of the calculations. In fact, in Fig. 4.1 we report the dependence of the ground state energy on the number of modes used to diagonalize H_r for different values of the strength interaction g . Obviously, the energy decreases as the number of modes increases reaching in all cases a limit saturating value with the number of modes which defines an asymptotic value. The horizontal line at $E_{gs} = 3/2$ corresponds to the ground-state energy of H_r in the limit $g \rightarrow \infty$. For any finite value of g one can always find a number of modes (m_{crit}) such that for a larger number of modes the energy will be always below $3/2$. The m_{crit} becomes larger as g increases. Therefore, one can conclude that when $g \rightarrow \infty$ the ground-state energy of H_r , as a function of the number of modes, approaches $3/2$ from below. For the case of two bosons trapped in a harmonic oscillator potential, we could have used the exact solutions of Ref. [14]. Instead we have decided to present a procedure which, although more tedious for this precise case, is more general and can readily be applied to other

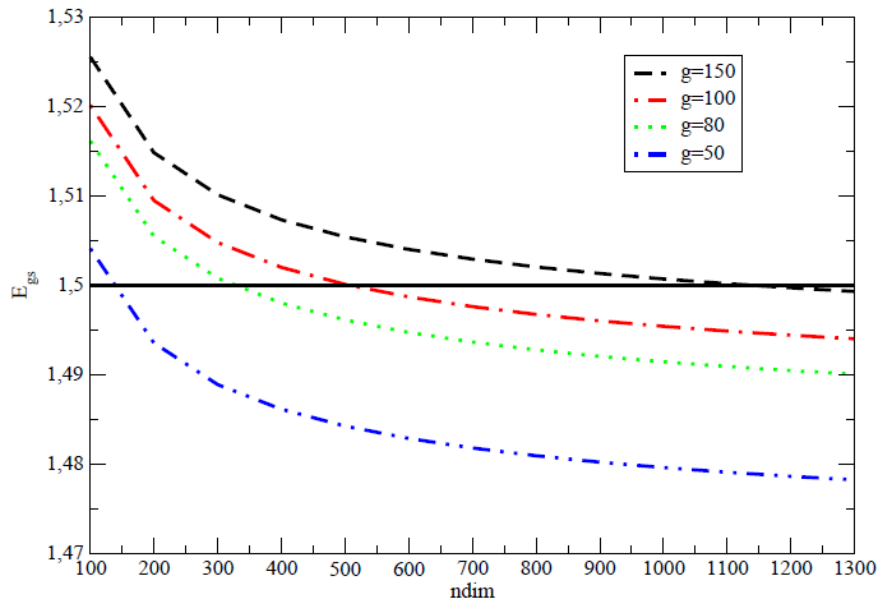


FIGURE 4.1: Ground state energy (in h.o. units) of H_r as a function of the number of modes (the dimension of the space used to diagonalize the Hamiltonian) for several values of the strength of the interaction.

single particle trapping potential besides the harmonic oscillator or also to other interactions by a proper computation of the matrix elements. Our results coincide, when applicable, with the exact solutions of Ref. [14].

4.5 Energy spectrum

The full spectrum of the problem will be obtained as,

$$E_{k,l} = E_k^{CM} + \bar{E}_l^{(r)}. \quad (4.13)$$

In Fig. 4.2 we depict the lowest part of the spectrum as a function of g . The eigenvalues are seen to evolve from the non-interacting bosonic system to those of a free fermionic system for $g \rightarrow \infty$. The g.s. of H is non-degenerated. At $g = 0$ is built with both atoms in the ground-state of the harmonic oscillator single-particle Hamiltonian or which is the same, it is the product of the ground-states of H_{CM} and H_r . Therefore both descriptions provide the same energy, $E = 1$.

However, in the limit $g \rightarrow \infty$, the ground state of the two-body system is given by the absolute value of the Slater determinant built with one atom in the ground state and the other in the first excited state of the harmonic oscillator single particle Hamiltonian. Therefore in this limit, the ground state energy (2 in h.o. units) is the sum of $1/2$ and $3/2$ single-particle energies, and the contribution of the contact interaction is zero. When one does the decomposition in H_{CM} and H_r the ground state in the $g \rightarrow \infty$ is achieved by taking the center of mass in the ground state ($\phi_0(X)$), i.e.

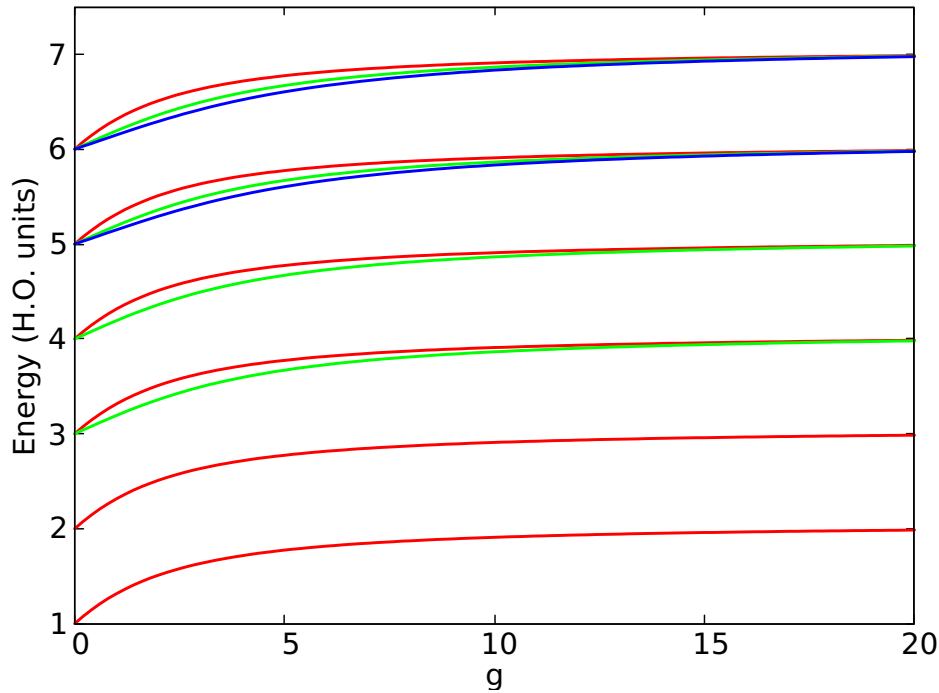


FIGURE 4.2: Lowest energy levels of the spectrum for the two bosons system, for a range of interaction strength $[0,20]$. The red lines correspond to the G.S. of H_r , whereas the green and blue lines correspond to its 1st and 2nd excitations respectively. These relative Hamiltonian states are also combined with C.M. excitations, which result in parallel curves which are shown with the same color for the same relative Hamiltonian state. For instance, the lowest state takes into account the energy of the ground state of the C.M., equal to $1/2$ and independent of the strength of the interaction, and the ground state energy of H_r which is $1/2$ for $g = 0$ and approaches $3/2$ for $g \rightarrow \infty$.

in the lowest CM level, with energy $1/2$, and the relative wave function is taken to be the absolute value of the first excited state, $\psi_1(x_r)$ of $H_r^{(0)}$ with energy $3/2$. Notice that $\psi_1(x_r)$ is an odd function and therefore it would be necessary to use an infinite basis of even functions, which are the ones that we have used in the diagonalization of H_r to respect the symmetry requirements for bosons, to asymptotically approach the exact eigenstate. The lowest excited state of the system corresponds to the first excitation of H_{CM} , with energy $3/2$ and to the relative ground state along g . Thus the first excited state has a constant excitation energy independent of g . Actually, the excitations of the c.m. show all the way up resulting in a set of curves parallel to the ground state curve, all depicted with red colour in Fig. 4.2. Notice that the first excited state at $g = 0$ can also be described as a properly symmetrized wave function with an atom in the ground state (energy $1/2$) and the other in the first excited state (energy $3/2$) of the single-particle harmonic oscillator Hamiltonian.

The next excitation consists of two states, one (red line) corresponds to 2 quanta of excitation of the C.M. motion, combined with the G.S. of H_r . While the

second (green line) describes the state, where the C.M. is in the ground state and the relative motion corresponds to the first excited state of positive parity of H_r . The two lines coincide at $g = 0$, where the energy level has degeneracy 2, then as g increases, the degeneracy is broken (green line) and the energy of this state is always below the energy of the state with two quanta of excitation of the C.M. At $g \rightarrow \infty$ the two states become again degenerated with total energy 4.

4.6 Contributions to the total energy

The transition from the BEC regime into a correlated one, finalizing at the Tonks-Girardeau regime, as the interaction strength is increased can be clearly seen in Fig. 4.3. There we report as a function of g the total g.s. energy (red line) decomposed in kinetic energy E_{kin} (blue line), harmonic oscillator potential energy V_{ho} (black line) and the interaction energy V_{int} (green line). Notice that both E_{kin} and V_{ho} contain a constant contribution of the C.M. equal to $1/4$. We observe how the interaction energy increases as g is increased until it reaches a maximum value around $g \simeq 2$. For $g \gtrsim 2$ the behavior changes completely and despite the atom-atom interaction strength is increased the interaction energy of the ground state decreases monotonically as $g \rightarrow \infty$. This is a clear consequence of the formation of correlations in the system which avoid the contact of the two bosons, much in line with systems like electrons in a 2D fractional Hall regime. Notice, that the exact wave function, when $g \rightarrow \infty$ for the relative motion, built as $|\psi_1(x_r)|$, does not feel the interaction. In fact, at $g = 0$, $V_{int} = 0$ and is zero again in the limit $g \rightarrow \infty$. The V_{ho} increases monotonically from $V_{ho} = 1/2$ at $g = 0$ up to $V_{ho} = 1$ for $g \rightarrow \infty$, While the kinetic energy starts at $E_{kin} = 1/2$ for $g = 0$, decreases a little bit, goes through a minimum and then starts to grow up to the value $E_{kin} = 1$ in the limit $g \rightarrow \infty$. For any value of g , the virial theorem

$$2E_{kin} - 2V_{ho} + V_{int} = 0 \quad (4.14)$$

is exactly fulfilled, indicating a good convergence of the energy results with the number of modes. The virial relation, together with the fact that $E = E_{kin} + V_{ho} + V_{int}$ allows to write

$$E_{kin} = \frac{1}{2}E - \frac{3}{4}V_{int}, \quad V_{ho} = \frac{1}{2}E - \frac{1}{4}V_{int} \quad (4.15)$$

which is valid for any value of g . Therefore we conclude that for any value of g , $V_{ho} \geq E_{kin}$. In particular, for $g = 0$, as $V_{int} = 0$, $E_{kin} = V_{ho} = e/2 = 1/2$. The same happens at $g \rightarrow \infty$ when $V_{int} = 0$, but with a different value of e , which turns to be $E/2 = 1$. In order to understand the behaviour of the different pieces of the energy, for very small g , we can combine a first order perturbation theory with the virial theorem. The correction to the energy is provided by the expectation value $V_{int,0} = \langle \phi_r^{(0)} | g\delta(x_r) | \phi_r^{(0)} \rangle = g\phi_r^{(0)}(0)\phi_r^{(0)}(0) = g\left(\frac{1}{2\pi}\right)^{1/2}$, where $|\phi_r^{(0)}\rangle$ is the ground state of $H_r^{(0)}$. Therefore, $V_{int,0}$ increases linearly with g . Using the previous relations for E_{kin} and V_{ho} ,

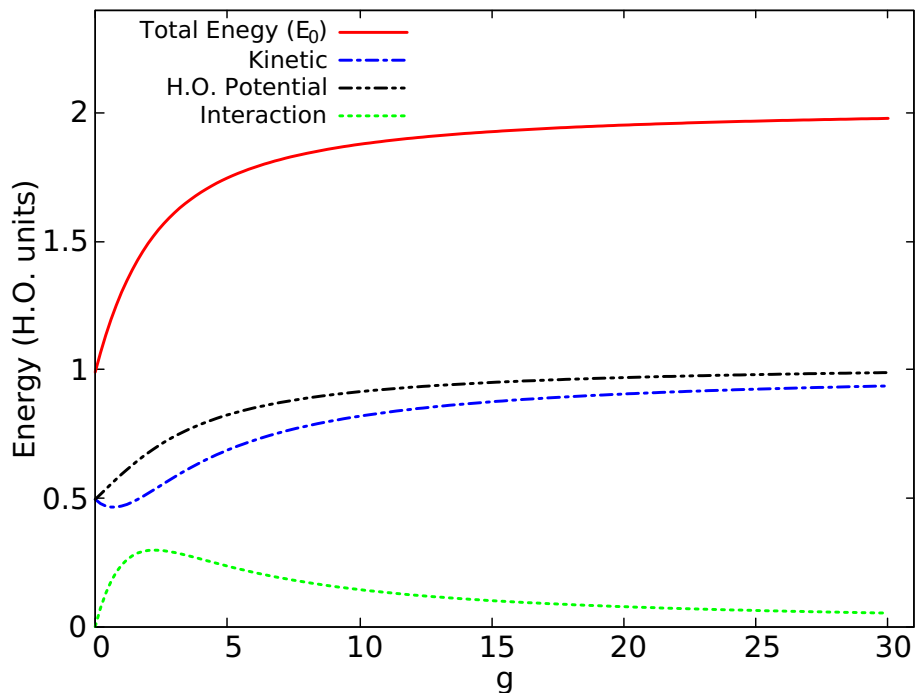


FIGURE 4.3: Different contributors to the ground state energy: $V_{H.O.}$, E_{kin} and V_{int} , shown in black, blue and green respectively. The total ground state energy is shown in red.

$$\begin{aligned}
 E_{kin} &= \frac{1}{2} - \frac{1}{4}V_{int,0} = \frac{1}{2} - \frac{1}{4}g \left(\frac{1}{2\pi} \right)^{1/2} \\
 V_{ho} &= \frac{1}{2} + \frac{1}{4}V_{int,0} = \frac{1}{2} + \frac{1}{4}g \left(\frac{1}{2\pi} \right)^{1/2}
 \end{aligned}
 \tag{4.16}$$

Therefore, for very small g the kinetic energy decreases while the harmonic oscillator energy increases with opposite slopes. These variations are associated to the kinetic and harmonic potential energies of the relative motion.

Chapter 5

Breathing mode

The natural way to explore the structure of a quantum system is to study the response of the system to excitations. Once we know the excitation operator, the response is mathematically expressed in terms of the Dynamic Structure Function. In this chapter we consider the monopole excitation operator which excites the so called breathing mode. For this excitation operator, the excitations can be separated in two types: center of mass excitations and intrinsic excitations. The lowest intrinsic excitation which corresponds to the breathing mode concentrates most of the strength of the dynamic structure.

5.1 Dynamic Structure Function (DSF): Excitation operator

The dynamic structure function encodes the response of our system to an external perturbation. In this section we will consider the dynamic structure function of a mono-polar excitation, also known as the breathing mode. For a system with an arbitrary number of particles N , the breathing mode can be excited by the one body operator,

$$\hat{F} = \sum_{i=1}^N x_i^2. \quad (5.1)$$

The associated Dynamic Structure Function reads

$$S_F(E) = \frac{1}{N} \sum_{a=0}^D \left| \langle a | \hat{F} | 0 \rangle \right|^2 \delta [E - (E_a - E_0)]. \quad (5.2)$$

in which d is the dimension of the truncated space of the diagonalization and where $|a\rangle$ runs over the excited states, $H |a\rangle = E_a |a\rangle$ and $|0\rangle$ is the ground state of the system. $S_F(E)$ can be explicitly computed with the eigen energies and eigenfunctions of the system.

5.2 Calculations for $N=2$

The monopole excitation operator $\hat{F} = \sum_{i=1}^N x_i^2$ can be separated in two pieces, one that corresponds to the center of mass and the other to the intrinsic motion. In the particular case of $N = 2$ we have,

$$\hat{F} = x_1^2 + x_2^2 = 2X^2 + \frac{x_r^2}{2}, \quad (5.3)$$

so that we compute the matrix elements $\langle a | \hat{F} | 0 \rangle$ taking advantage of the factorization of the state, $|a\rangle = |\lambda_{CM}\rangle |\nu_r\rangle = |\Phi_{CM}^\lambda\rangle |\Phi_r^\nu\rangle$, where λ & ν are the quantum numbers associated to the C.M. and the relative part of the state $|a\rangle$ of our system

$$\begin{aligned} \langle a | \hat{F} | 0 \rangle &= \langle \Phi_{CM}^\lambda | \langle \Phi_r^\nu | \left[2X^2 + \frac{x_r^2}{2} \right] | \Phi_{CM}^0 \rangle | \Phi_r^0 \rangle \\ &= \langle \Phi_{CM}^\lambda | 2X^2 | \Phi_{CM}^0 \rangle \langle \Phi_r^\nu | \Phi_r^0 \rangle + \langle \Phi_r^\nu | \frac{x_r^2}{2} | \Phi_r^0 \rangle \langle \Phi_{CM}^\lambda | \Phi_{CM}^0 \rangle. \end{aligned} \quad (5.4)$$

The product $\langle \Phi_{CM}^\lambda | 2X^2 | \Phi_{CM}^0 \rangle$ can be obtained using the orthogonality properties of the Hermite's polynomials in the following way: First of all we write the product explicitly

$$\begin{aligned} \langle \Phi_{CM}^\lambda | 2X^2 | \Phi_{CM}^0 \rangle &= \int_{-\infty}^{\infty} \Psi^{\lambda*}(X) 2X^2 \Psi_0(X) dX \\ &= \left(\frac{2}{\pi} \right)^{1/2} \frac{1}{\sqrt{2^\lambda \lambda!}} \int_{-\infty}^{\infty} H_\lambda(\sqrt{2}X) e^{-X^2/2} 2X^2 H_0(\sqrt{2}X) e^{-X^2/2} dX \\ &= \left(\frac{2}{\pi} \right)^{1/2} \frac{1}{\sqrt{2^\lambda \lambda!}} \int_{-\infty}^{\infty} H_\lambda(\sqrt{2}X) e^{-X^2} 2X^2 dX. \end{aligned} \quad (5.5)$$

After that, we can perform a variable change $y \equiv \sqrt{2}X$ obtaining

$$\langle \Phi_{CM}^\lambda | 2X^2 | \Phi_{CM}^0 \rangle = 2 \left(\frac{2}{\pi} \right)^{1/2} \frac{1}{\sqrt{2^\lambda \lambda!}} 2^{-3/2} \int_{-\infty}^{\infty} H_\lambda(y) e^{-y^2} y^2 dy \quad (5.6)$$

and taking advantage of the fact that y^2 can be expressed in terms of the Hermite's Polynomials, we can use

$$H_2(y) = 4y^2 - 2 = 4y^2 - 2H_0(y) \Rightarrow y^2 = \frac{H_2(y)}{4} + \frac{H_0(y)}{2}, \quad (5.7)$$

to rewrite the eq. (5.6)

$$\langle \Phi_{CM}^\lambda | 2X^2 | \Phi_{CM}^0 \rangle = 2 \left(\frac{2}{\pi} \right)^{1/2} \frac{1}{\sqrt{2^\lambda \lambda!}} 2^{-3/2} \int_{-\infty}^{\infty} H_\lambda(y) e^{-y^2} \left(\frac{H_2(y)}{4} + \frac{H_0(y)}{2} \right) dy. \quad (5.8)$$

We have used that the integral value will be the same for y_1 and y_2 , as we integrate over all the space, in order to do the summation. Then, using the orthogonality properties, we do know

$$\int_{-\infty}^{\infty} e^{-x^2} H_{\alpha}(x) H_{\beta}(x) dx = \sqrt{\pi} 2^{\alpha} \alpha! \delta_{\alpha,\beta}. \quad (5.9)$$

Finally, we observe that the only possible values of λ for the C.M. contribution to the breathing mode are 0 and 2

$$\begin{aligned} \langle \Phi_{CM}^{\lambda} | 2X^2 | \Phi_{CM}^0 \rangle &= 2 \left(\frac{2}{\pi} \right)^{1/2} \frac{1}{\sqrt{2^{\lambda} \lambda!}} 2^{-3/2} \left(\frac{\sqrt{\pi} 2^{2\lambda} 2!}{4} \delta_{2,\lambda} + \frac{\sqrt{\pi}}{2} \delta_{0,\lambda} \right) \\ &= \frac{4\delta_{2,\lambda} + \delta_{0,\lambda}}{2 \cdot \sqrt{2^{\lambda} \lambda!}}. \end{aligned} \quad (5.10)$$

As we have diagonalized the relative Hamiltonian the eigenstates obtained are orthogonal, and orthonormal when normalized, and consequently we can obtain the matrix elements $\langle \Phi_r^{\nu} | \Phi_r^0 \rangle$ as

$$\langle \Phi_r^{\nu} | \Phi_r^0 \rangle = \delta_{\nu,0}. \quad (5.11)$$

With all this, we observe that the contribution of the C.M. operator to the breathing mode is very limited, since only accepts two possible states, corresponding to $\lambda = 0, 2$ as explained above. On the other hand, the H_r will contribute to the breathing mode very differently. As we are using many H.O. states to diagonalize and obtain our eigenstates, every excited state will connect many H.O. states by pairs, as we are going to demonstrate.

First of all, we obtain $\langle \Phi_{CM}^{\lambda} | \Phi_{CM}^0 \rangle = \delta_{\lambda,0}$ simply because of the normalization of the wave-function in the H.O. that describes the C.M. motion

$$\langle \Phi_r^{\nu} | \frac{x_r^2}{2} | \Phi_r^0 \rangle \langle \Phi_{CM}^{\lambda} | \Phi_{CM}^0 \rangle = \langle \Phi_r^{\nu} | \frac{x_r^2}{2} | \Phi_r^0 \rangle \delta_{\lambda,0}. \quad (5.12)$$

Then, as the states $|\Phi_r\rangle$ are linear combinations of all the eigenstates of a H.O. system, the matrix elements $\langle \Phi_r^{\nu} | \frac{x_r^2}{2} | \Phi_r^0 \rangle$ must be expressed in terms of H.O. matrix elements in the following way

$$\begin{aligned} |\Phi_r^{\nu}\rangle &= \sum_{\alpha} C_{\alpha}^{\nu} |\Phi_{\alpha}^{H.O.}\rangle \\ \langle \Phi_r^{\nu} | \frac{x_r^2}{2} | \Phi_r^0 \rangle &= \sum_{\alpha,\beta} \frac{C_{\alpha}^{\nu} C_{\beta}^0}{2} \langle \Phi_{\alpha}^{H.O.} | x_r^2 | \Phi_{\beta}^{H.O.} \rangle, \end{aligned} \quad (5.13)$$

where the matrix elements $\langle \Phi_{\alpha}^{H.O.} | x_r^2 | \Phi_{\beta}^{H.O.} \rangle$ can be expressed as a solvable integral which solution is

$$\langle \Phi_{\alpha}^{H.O.} | x_r^2 | \Phi_{\beta}^{H.O.} \rangle = \begin{cases} \frac{\sqrt{\beta(\beta-1)}}{2a_r} & \alpha = \beta - 2 \\ \frac{2\beta+1}{2a_r} & \alpha = \beta \\ \frac{\sqrt{(\beta+1)(\beta+2)}}{2a_r} & \alpha = \beta + 2 \\ 0 & \text{Otherwise.} \end{cases} \quad (5.14)$$

Using these integral solutions, we can rewrite the breathing mode operator's mean value as

$$\begin{aligned} \langle a | \hat{F} | 0 \rangle &= \langle \Phi_{CM}^\lambda | 2X^2 | \Phi_{CM}^0 \rangle \langle \Phi_r^\nu | \Phi_r^0 \rangle + \langle \Phi_r^\nu | \frac{x_r^2}{2} | \Phi_r^0 \rangle \langle \Phi_{CM}^\lambda | \Phi_{CM}^0 \rangle \\ &= \frac{4\delta_{\lambda,2} + \delta_{\lambda,0}}{2 \cdot \sqrt{2^\lambda \lambda!}} \delta_{\nu,0} + \sum_{\alpha,\beta} \frac{C_\alpha^\nu C_\beta^0}{2} \langle \Phi_\alpha^{H.O.} | x_r^2 | \Phi_\beta^{H.O.} \rangle \delta_{\lambda,0}. \end{aligned} \quad (5.15)$$

Notice that actually, we have clearly two contributions to the DSF; the first one corresponds to the C.M., and can only connect the ground state with the first excitation of the C.M. However, in the second contribution, which belongs to the relative Hamiltonian excitations, we are able to connect many H.O. states since the relative motion states are not pure H.O. states. Therefore, if we want to depict the exact value, we just need to use this formula in the eigenstates diagonalized above.

5.3 Results for two particles

For $g = 0$ and $g \rightarrow \infty$ we can also compute $S_F(E)$ analytically. In the case of $g = 0$ both contributions of the excitation operator, i.e. C.M. and intrinsic, excite only two different states, both at the same energy $E = 2$, being both strengths the center of mass excitation and the one of the relative motion $1/4$. The C.M. peak will remain at the same energy and with the same strength independently of the interaction strengths. In the $g \rightarrow \infty$ case the two excitations are again peaked at $E = 2$ but they have different strengths, $1/4$ for the C.M. and $3/4$ for the internal excitation. This implies that even though both excitations have exactly the same energy it should be more likely to excite the breathing mode in the TG limit than in the BEC one.

In Fig. 5.1 we depict the strengths of the dynamic structure function for $N = 2$ for four different values of the interaction g . Notice that the strength contains the factor $1/N$ included in the definition of $S_F(E)$. For $g = 0$, we have only one peak, corresponding to the sum of the C.M. and relative motion. As mentioned before, the C.M. peak will remain constant within for all the interaction strengths.

For nonzero values of the interaction, the strength is distributed over several excited states, but in all cases the center of mass peak remains visible and located at $E = 2$. The strength of the higher intrinsic peaks is always significantly smaller, two orders of magnitude, than those of the center of mass and the breathing mode. The strength of the breathing mode and the next three excited states of the relative motion is shown in Fig. 5.2 as a function of g . In all cases, at $g = 0$, the strength of these secondary peaks is zero, and increases with g up to a maximum located around $g \approx 2$, and decreases to zero for $g \rightarrow \infty$. The maximum decreases when the excitation energy increases. Apparently, this dependence is very much correlated to the dependence of the interaction energy with g (Fig. 4.3). In Fig. 5.2 we report the dependence of the strength of the breathing mode as a function of g , which turns out to be an increasing function of g . This behavior will be relevant to understand the evolution of the energy weighted sum rules of $S_F(E)$.

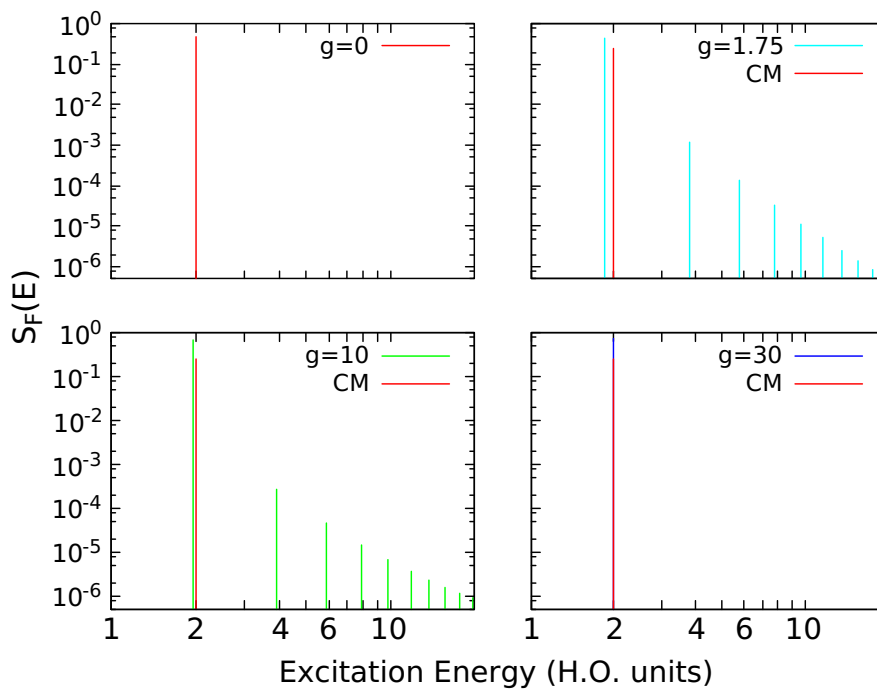


FIGURE 5.1: Dynamic structure function computed for a system composed by 2 bosons, with a delta contact potential. The value is computed for different interaction's g values [0,30], and with a number of modes $m=200$ (101 modes).

The breathing mode energy decreases (it lies below the C.M. excitation) for increasing g up to $g \lesssim 2$, above that, it increases again towards $E = 2$ when $g \rightarrow \infty$. This is the so called reentrant behavior of the mono-polar excitation reported in Ref. [23]. In an experiment, separating the contribution from the center of mass from that of the breathing mode seems involved. The response of the system will thus easily mix both contributions.

The reentrant behavior affects not only to the ground state but to all excited states of the relative motion. The reentrant energy, defined as $E_r = Ex(g) - Ex(g = 0)$ is zero, by definition, at $g = 0$, it decreases reaching a negative minimum and then grows to approach asymptotically zero when $g \rightarrow \infty$. The reentrant behaviour is more pronounced for the higher excited states. The maximum reentrance slightly shifts to higher values of g for the higher excited states. Again, there seems to exist a correlation between the interaction energy and the reentrant energy as a function of g . Computing the structure function explicitly becomes difficult for more than 2 particles. In particular a naive second quantization scheme using the one particle modes as single particle states runs into difficulties as it mixes the center of mass with the relative motion in a nontrivial way [24].

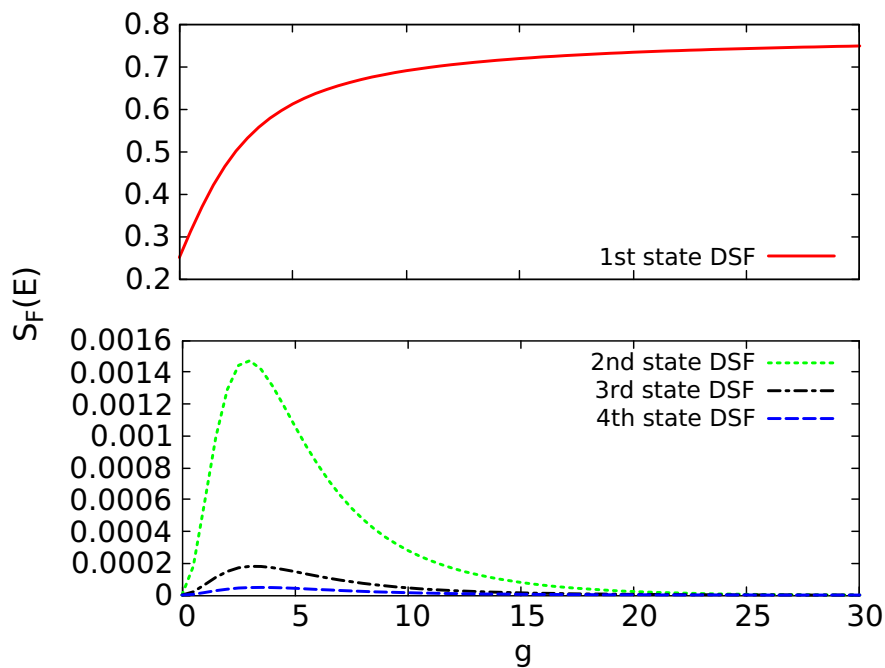


FIGURE 5.2: Strength of excitations of H_r as a function of g . The breathing mode can be observed in red, whereas the other three excited states are shown in green, black and blue, respectively. The breathing mode is at least two orders of magnitude more intense than the other excitations in the whole range of interaction strength $[0,30]$.

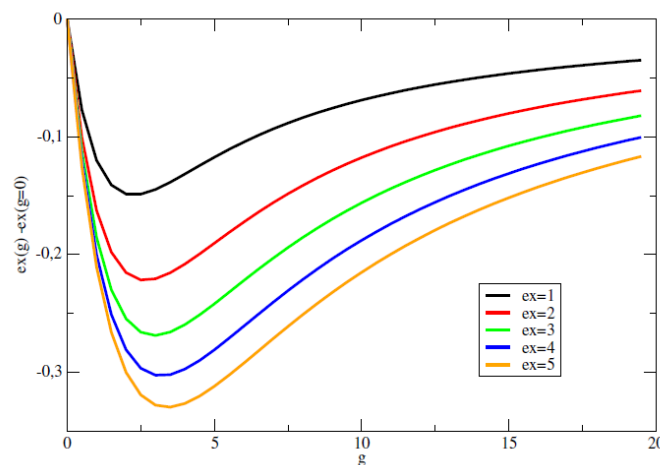


FIGURE 5.3: Reentrant energy, $Ex(g) - Ex(g = 0)$ as a function of the strength of the interaction for several excited states of the relative motion.

5.4 Excitation of the C.M.

For the monopole operator, the contribution of the C.M. piece of the excitation operator can be exactly calculated for any number of particles. In fact, starting from the

definition of the DSF

$$S_F(E) = \frac{1}{N} \sum_j |\langle j | \sum_{i=1}^N x_i^2 | 0 \rangle|^2 \delta(E - (E_j - E_0)), \quad (5.16)$$

where $|j\rangle$ is a general excited state of the system. However, the excited states can be factorized $|j\rangle = |j_{CM}\rangle |j_{rel}\rangle$ and the excitation operator can be also splitted into two pieces, in such a way that the matrix elements responsible of the DSF can be written as:

$$\langle j | \sum_i x_i^2 | 0 \rangle = \langle j_{CM}, j_r | NX^2 + \frac{1}{N} \sum_{i<j} (x_i - x_j)^2 | 0_{CM}, 0_r \rangle \quad (5.17)$$

which can be expressed as

$$\langle j | \sum_i x_i^2 | 0 \rangle = \langle j_{CM} | NX^2 | 0_{CM} \rangle \langle j_r | 0_r \rangle + \langle j_{CM} | 0_{CM} \rangle \langle j_r | \frac{1}{N} \sum_{i<j} (x_i - x_j)^2 | 0_r \rangle. \quad (5.18)$$

Taking into account the orthogonality of the states, it can be rewritten:

$$\langle j | \sum_i x_i^2 | 0 \rangle = \langle j_{CM} | NX^2 | 0_{CM} \rangle \delta_{j_r, 0_r} + \delta_{j_{CM}, 0_{CM}} \langle j_r | \frac{1}{N} \sum_{i<j} (x_i - x_j)^2 | 0_r \rangle. \quad (5.19)$$

Therefore, we have separated the excitations of the C.M. from the intrinsic excitations for the general case of N particles. Now, we should take into account that the spectrum of the C.M. is identical to the harmonic oscillator: $1/2, 3/2, 5/2, \dots$ and that the ground state will correspond always to the $j_{CM} = 0$ state with energy $1/2$. With this excitation operator, the only excitation of the C.M. will correspond always to excite the state $j_{CM} = 2$ with energy $E_{CM} = 5/2$, with an excitation energy $E_{exc}^{CM} = 2$. The matrix element, for $j_{CM} \neq 0$ fulfills that:

$$\langle j_{CM} | NX^2 | 0_{CM} \rangle = \delta_{j_{CM}, 2} N \langle 2_{CM} | X^2 | 0_{CM} \rangle. \quad (5.20)$$

Actually, one can evaluate this matrix element so that

$$\langle 2_{CM} | X^2 | 0_{CM} \rangle = \frac{1}{\sqrt{2}N}, \quad (5.21)$$

and

$$|\langle j_{CM} | NX^2 | 0_{CM} \rangle|^2 = \left| N \frac{1}{\sqrt{2}N} \right|^2 = \frac{1}{2}. \quad (5.22)$$

The C.M. excitation appears always at an excitation energy $E = 2$ with strength $\frac{1}{2N}$, independently of the interactions between the particles. The factor $\frac{1}{N}$ is due to our definition of $S_F(E)$ in 5.16. Also notice that this is an alternative and more generalist way to obtain 5.10.

Chapter 6

Sum Rules

In this chapter we introduce the energy sum rules of the dynamic structure function associated to a given excitation operator. The sum rules encode the response of the system to an excitation, in particular we focus our attention on the mono-polar excitation. We derive explicitly and with complete generality for the sum rules M_{-1} , M_1 and M_3 for N particle systems. The most important outcome from these sum rules is that they allow us to compute an estimate of the main excitation energy of the system, i.e., the breathing mode energy in our case, by only knowing some properties of the ground state of the system.

6.1 The energy sum rules

The energy moments (M_n) of the dynamic structure function associated to a given excitation operator \hat{F}

$$\begin{aligned} M_n(E) &= \int_0^\infty E^n S_F(E) dE \\ &= \frac{1}{N} \sum_a (E_a - E_0)^n \left| \langle a | \hat{F} | 0 \rangle \right|^2. \end{aligned} \quad (6.1)$$

provide a full characterization of the response of the system.

If the dynamic structure function is concentrated around a single excitation energy, $S_F \simeq S_m \delta(E - E_{ex})$, then a few energy moments are enough to reconstruct the DSF. In this extreme case, we have $E_{ex} \simeq \sqrt{M_n/M_{n-2}}$. For instance, the simplest one would be $E_{ex} \simeq \sqrt{M_1/M_{-1}}$. Usually, the DSF associated to a given operator \hat{F} is difficult to calculate. It turns out, however, that the energy moments of the DSF, can be calculated without the explicit knowledge of the DSF.

As it is well known, there is a great number of theorems that allow one to compute several of the M_n without any explicit knowledge of all the eigenvalues and eigenvectors of the many-body systems [25]. This is done through so-called *Sum Rules*. These sum rules can be computed by the expectation values on the ground state of certain suitable operators. This strategy is specially appropriate when we have a good knowledge of the ground-state of the system, and is the way that Monte-Carlo calculations take advantage of its capability to calculate the ground

state properties for large number of particles to provide information on the response of the system [23].

In this chapter we derive the M_{-1} , M_{-1} and M_{-3} energy sum rules associated to the single-particle operator \hat{F} . Some of the derivations are valid for any excitation operator but finally we give the explicit results for $\hat{F} = \sum_i x_i^2$. The derivation is valid for any number of particles and in some aspects applies to any inter-particle interaction. However, at the end we report the results for $N = 2$ and for the contact interaction. The contribution of the C.M. motion to the considered sum rules is also discussed.

6.2 Derivation of the sum rules

In this section we will derive the sum rules M_{-1} , M_1 and M_3 with complete generality. These sum rules can be applied to any system of N particles, either they are fermions or bosons, with a Hamiltonian of the kind from 3.2.

6.2.1 M_{-1} sum rule

The sum rule M_{-1} can be obtained through perturbation theory, by defining a new Hamiltonian as $\hat{H}' = \hat{H} + \lambda\hat{F}$, where \hat{H} is the unperturbed Hamiltonian with an unperturbed ground state energy E_0 , and $\lambda\hat{F}$ is the perturbation, which in our case is $\hat{F} = \sum_i x_i^2$. The expansion of the energy up to the second order, can be written as

$$E_0(\lambda) = E_0 + \lambda \langle 0 | \hat{F} | 0 \rangle + \lambda^2 \sum_q \frac{|\langle q | \hat{F} | 0 \rangle|^2}{E_0 - E_q}, \quad (6.2)$$

and therefore the M_{-1} sum rule can be obtained as

$$M_{-1} = -\frac{1}{2} \frac{1}{N} \left. \frac{\partial^2 E_0(\lambda)}{\partial \lambda^2} \right|_{\lambda=0}, \quad (6.3)$$

which can be calculated numerically.

Alternatively, related with this procedure, we have another way to calculate this sum rule, which can be used as a test

$$M_{-1} = -\frac{1}{2} \frac{1}{N} \left. \frac{d}{d\lambda} \langle \tilde{0} | F | \tilde{0} \rangle \right|_{\lambda=0}, \quad (6.4)$$

where $|\tilde{0}\rangle$ is the ground state of $H + \lambda F$. In fact, the expansion of the ground state of $H + \lambda F$ around $\lambda = 0$ can be written as

$$|\tilde{0}\rangle = |0\rangle + \lambda \sum_{k \neq 0} \frac{F_{k0}}{E_0 - E_k} |k\rangle + \dots, \quad (6.5)$$

and

$$\langle \tilde{0} | F | \tilde{0} \rangle = \langle 0 | F | 0 \rangle + 2\lambda \sum_{k \neq 0} \frac{|\langle k | F | 0 \rangle|^2}{E_0 - E_k} + \dots \quad (6.6)$$

Therefore,

$$\left. \frac{d(\langle \tilde{0} | F | \tilde{0} \rangle)}{d\lambda} \right|_{\lambda=0} = 2 \sum_{k \neq 0} \frac{|\langle k | F | 0 \rangle|^2}{E_0 - E_k}, \quad (6.7)$$

and recovering expression 6.4

$$M_{-1} = -\frac{1}{2} \frac{1}{N} \frac{d}{d\lambda} \langle \tilde{0} | F | \tilde{0} \rangle \Big|_{\lambda=0}. \quad (6.8)$$

6.2.2 M_1 sum rule

Using the definition of M_1 , one can express the sum rule as the expectation value of a certain commutator of the excitation operator \hat{F} and the Hamiltonian in the ground-state of the system.

$$\begin{aligned} M_1 &= \int ES_F(E)dE = \frac{1}{N} \int dEE \sum_n |\langle n | F | 0 \rangle|^2 \delta(E - (E_n - E_0)) \\ &= \frac{1}{N} \sum_n (E_n - E_0) \langle 0 | F^\dagger | n \rangle \langle n | F | 0 \rangle \\ &= \frac{1}{N} \sum (\langle 0 | F^\dagger | n \rangle \langle n | E_n F | 0 \rangle - \langle 0 | F^\dagger | n \rangle \langle n | F E_0 | 0 \rangle) \quad (6.9) \\ &= \frac{1}{N} \sum (\langle 0 | F^\dagger | n \rangle \langle n | HF | 0 \rangle - \langle 0 | F^\dagger | n \rangle \langle n | FH | 0 \rangle) \\ &= \frac{1}{N} \langle 0 | F^\dagger [H, F] | 0 \rangle = \frac{1}{2} \frac{1}{N} \langle 0 | [F^\dagger, [H, F]] | 0 \rangle. \end{aligned}$$

With this new expression we are able to compute M_1 using only the ground state. To do so, we must start computing the commutators for the specific $\hat{F} = \sum_i x_i^2$,

$$[H, F] = [E_{kin} + V_{H.O.} + V_{int}, F] = [E_{kin}, F] + [V_{H.O.}, F] + [V_{int}, F]. \quad (6.10)$$

Since both potentials $V_{H.O.}$ and V_{int} depend only on the coordinates, we have that $[V_{H.O.}, F] = [V_{int}, F] = 0$. Therefore, we only need to calculate the kinetic energy commutator

$$[E_{kin}, F] = - \left[\sum_{i=1}^N \frac{1}{2} \frac{d^2}{dx_i^2}, \sum_{j=1}^N x_j^2 \right] = -\frac{1}{2} \sum_{i,j} \left[\frac{d^2}{dx_i^2}, x_j^2 \right] \delta_{i,j} = -\frac{1}{2} \sum_{i=1}^N \left[\frac{d^2}{dx_i^2}, x_i^2 \right]. \quad (6.11)$$

In order to evaluate these commutators we must use the canonical commutation rules

$$p = -i \frac{d}{dx}, \quad \left[-i \frac{d}{dx}, x \right] = [p, x] = -i, \quad (6.12)$$

and the property $[AB, C] = A[B, C] + [A, C]B$. Therefore, applying both

$$\begin{aligned} \left[-\frac{d^2}{dx_i^2}, x_i^2 \right] &= [p^2, x^2] = p [p, x^2] + [p, x^2] p \\ &= p [p, x] x + px [p, x] + [p, x] xp + x [p, x] p \\ &= -i(px + px + xp + xp) = -2i(px + xp). \end{aligned} \quad (6.13)$$

With this expression, the commutator can be written as it as

$$[H, F] = \frac{1}{2} \sum_{i=1}^N [p_i^2, x_i^2] = -i \sum_{i=1}^N (p_i x_i + x_i p_i), \quad (6.14)$$

and therefore,

$$\begin{aligned} [F^\dagger, [H, F]] &= \left[\sum_i x_i^2, -i \sum_j (p_j x_j + x_j p_j) \right] = -i \sum_i \sum_j [x_i^2, p_j x_j + x_j p_j] \\ &= -i \sum_j [x_j^2, p_j x_j + x_j p_j] = -i \sum_j ([x_j^2, p_j] x_j + p_j [x_j^2, x_j] + [x_j^2, x_j] p_j + x_j [x_j^2, p_j]) \\ &= -i \sum_j ([x_j^2, p_j] x_j + x_j [x_j^2, p_j]) \\ &= -i \sum_j (x_j [x_j, p_j] x_j + [x_j, p_j] x_j x_j + x_j x_j [x_j, p_j] + x_j [x_j, p_j] x_j) = -i \sum_j i4x_j^2. \end{aligned} \quad (6.15)$$

Introducing this result on the sum rule M_1 ,

$$M_1 = \frac{1}{2} \langle 0 | [F^\dagger, [H, F]] | 0 \rangle = \frac{2}{N} \langle 0 | \sum_{i=1}^N x_i^2 | 0 \rangle. \quad (6.16)$$

Taking into account the symmetry of the N-particle wave-function and that F is a one-body operator, the sum rule M_1 can be expressed as

$$M_1 = 2 \langle 0 | x^2 | 0 \rangle = 2 \int_{-\infty}^{\infty} x^2 \rho(x) dx = \frac{4}{N} \langle V_{H.O.} \rangle, \quad (6.17)$$

where the one-body density is normalized as $\int_{-\infty}^{\infty} \rho(x) dx = 1$.

6.2.3 M_3 sum rule

Assuming that \hat{F} is hermitian so that

$$[H, F]^\dagger = -[H, F] \quad (6.18)$$

the sum rule M_3 can be computed using the expectation value

$$M_3 = \frac{1}{2N} \langle 0 | [[H, F], [H, [H, F]]] | 0 \rangle . \quad (6.19)$$

Alternatively, it can also be computed as

$$M_3 = \frac{1}{2N} \left. \frac{\partial^2 E_\eta}{\partial \eta^2} \right|_{\eta=0}, \quad (6.20)$$

where

$$E_\eta = \langle \phi_\eta | H | \phi_\eta \rangle, \quad (6.21)$$

with

$$|\phi_\eta\rangle = e^{\eta[H, F]} |0\rangle. \quad (6.22)$$

Therefore, the first derivative is

$$\begin{aligned} \frac{dE_\eta}{d\eta} &= \langle 0 | -e^{-\eta[H, F]} [H, F] H e^{\eta[H, F]} + e^{-\eta[H, F]} H [H, F] e^{\eta[H, F]} | 0 \rangle \\ &= -\langle 0 | e^{-\eta[H, F]} [[H, F], H] e^{\eta[H, F]} | 0 \rangle, \end{aligned} \quad (6.23)$$

and the second derivative yields

$$\begin{aligned} \frac{d^2 E_\eta}{d\eta^2} &= \frac{d}{d\eta} \left(-\langle 0 | e^{-\eta[H, F]} [[H, F], H] e^{\eta[H, F]} | 0 \rangle \right) \\ &= \langle 0 | e^{-\eta[H, F]} [H, F] [[H, F], H] e^{\eta[H, F]} - e^{-\eta[H, F]} [[H, F], H] [H, F] e^{\eta[H, F]} | 0 \rangle \\ &= \langle 0 | e^{-\eta[H, F]} [[H, F], [H, [H, F]]] e^{\eta[H, F]} | 0 \rangle, \end{aligned} \quad (6.24)$$

and therefore M_3 it can be computed as

$$M_3 = \frac{1}{2N} \left. \frac{\partial^2 E_\eta}{\partial \eta^2} \right|_{\eta=0}. \quad (6.25)$$

Noticing that

$$e^{\eta[H, F]} \Psi(x_1, x_2, \dots, x_N) = \Psi(e^\eta x_1, e^\eta x_2, \dots, e^\eta x_N), \quad (6.26)$$

and recalling the virial theorem

$$E_\lambda = \langle \psi_\lambda | H | \psi_\lambda \rangle = \lambda^2 E_{kin}(\lambda = 1) - \frac{1}{\lambda^2} V_{HO}(\lambda = 1) + \lambda V_{int}(\lambda = 1), \quad (6.27)$$

where

$$\Psi_\lambda(x_1, x_2, \dots, x_N) = \lambda^{N/2} \Psi(\lambda x_1, \lambda x_2, \dots, \lambda x_N), \quad (6.28)$$

it is shown that for the monopole excitation,

$$M_3 = \frac{4}{N}(E_{kin} + 3V_{HO}) \quad (6.29)$$

6.3 Non-interacting and Tonks-Girardeau limits

The non-interacting and the infinitely interacting limits are particularly amenable and allow one to compute the exact limiting values of M_1 and M_3 sum rules. The two sum rules can be cast as a function of the average values of the kinetic and harmonic oscillator energies. The M_1 and M_3 sum rules for N particles read,

$$\begin{aligned} M_1 &= \frac{4}{N}V_{HO} \\ M_3 &= \frac{4}{N}(E_{kin} + 3V_{HO}) = \frac{16}{N}V_{HO}. \end{aligned} \quad (6.30)$$

For $g = 0$, all particles populate the H.O. single-particle ground state, therefore the total, kinetic and harmonic potential energy are , $E = N/2$, $E_{kin} = N/4$ and $V_{h.o.} = N/4$. Therefore, the estimate of the mono-polar excitation energy is

$$E_{exc} = \sqrt{\frac{M_3}{M_1}} = \sqrt{\frac{4V_{HO}}{V_{HO}}} = 2. \quad (6.31)$$

corresponding to the excitation of one particle in the second single-particle state of the H.O.

Surprisingly, in the TG limit we obtain the same result for the estimation of the excitation energy. To evaluate the sum rules in this limit we rely on the Bose-Fermi mapping. We have seen in a previous chapter that the total energy in the case of N particles is $E = N^2/2$. Then taking into account the virial theorem, valid also in this limit, we have that $E_{kin} = N^2/4$ and also $V_{h.o.} = N^2/4$. Therefore, $M_1 = 4V_{h.o.}/N = N$, and $M_3 = 4(E_{kin} + 3V_{h.o.})/N = 4N$ and therefore:

$$E_{ex} = \sqrt{\frac{M_3}{M_1}} = \sqrt{\frac{4N}{N}} = 2. \quad (6.32)$$

which is the same as in the non-interacting case.

It is also interesting to pay attention to the contribution of the C.M. excitation to the energy sum rules. We have already seen that the energy of the C.M. excitation lies 2 energy units above the ground state, independently of the number of particles, and the strength of the excitation is given by $1/(2N)$. Therefore, the contribution of

the C.M. to the total energy sum rules is

$$\begin{aligned}M_{-1,CM} &= \frac{1}{E_{ex}} \frac{1}{N} \frac{1}{2} = \frac{1}{4N} \\M_{1,CM} &= E_{ex} \frac{1}{N} \frac{1}{2} = \frac{1}{N} \\M_{3,CM} &= E_{ex}^3 \frac{1}{N} \frac{1}{2} = \frac{4}{N}\end{aligned}\tag{6.33}$$

After this analysis of the sum rules we are ready for the discussion of the $N = 2$ results that will be presented in the next chapter.

Chapter 7

Sum Rules applied to a 2 bosons system

In previous chapters, we have derived the sum rules with complete generality for N particles. We have also calculated the properties of the ground-state, excitation spectrum and the dynamic structure function associated to the monopole excitation for $N = 2$. The calculations for $N > 2$ for any values of g are much more involved. Although we have been able to provide some limiting values for two extreme cases: $g = 0$ and $g \rightarrow \infty$. As an alternative, we have proposed to use energy sum rules as a convenient method to estimate some average properties of the dynamical structure function. In this chapter we want to explore the limitations of the sum rules method by comparing with the explicit calculation of $S_F(E)$ and gain confidence on these sum rules for future works with $N > 2$.

7.1 Behaviour of the sum rules and contribution of the C.M. peak

We start our discussion by comparing in Fig.7.1 the results of the energy sum rules M_{-1} , M_1 and M_3 for different values of g calculated using the explicit values of $S_F(E)$ with the values obtained from the ground state properties. We can appreciate a very good agreement between the two ways to calculate the sum rules in all the range of g considered. Notice the importance of this comparison: using the $S_F(E)$ to compute the sum rules, we must know the whole spectrum (or at least the few more probable excited states, which here correspond to the lowest excited energy states), whereas using the sum rules relations we can calculate them by only using information about the ground state.

It should be mentioned that even if the higher peaks of $S_F(E)$ have a very small strength their contribution to the sum rules is not negligible. In particular for M_3 . In fact, one requires a very good precision in the calculation of the excitation energies and their strengths or equivalently a huge dimension of the Hilbert space when diagonalizing the Hamiltonian which increases when g is large. To cure this problem, we have performed the diagonalization using 101 modes and taking only the first ten excited states to compute the sum rules. This procedure provides stable results.

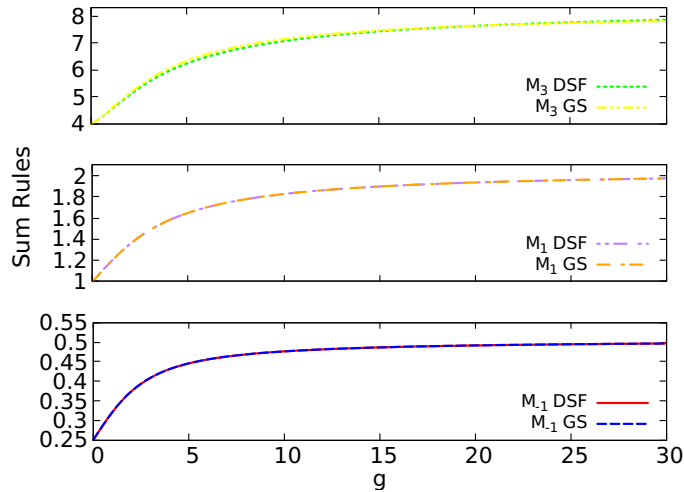


FIGURE 7.1: Comparison of the sum rules M_{-1} , M_1 and M_3 computed through the DSF or using the ground-state properties. In the DSF method we have truncated the spectra by taking the first 10 energy levels and both have been computed with $m=200$ (101 modes).

All the sum rules are increasing functions of the strength of the interaction and approach an asymptotic value for $g \rightarrow \infty$. The increasing character of the sum rules with g is mainly due to the increment of the strength of the breathing mode with g . As expected the convergence to the asymptotic values is faster for M_{-1} and slower for M_3 . However, in all cases for $g = 30$, the largest value of g considered in the figure, the convergence has been almost reached.

For $N = 2$, the expressions derived in the previous chapter in the non-interacting limit reduce to $M_1 = 1$ and $M_3 = 4$, while for the Tonks- Girardeau regime we have $M_1 = 2$ and $M_3 = 8$. Also relevant is the contribution of the C.M. excitation to the total sum rules, as mentioned before, the contribution is independent of g and for $N = 2$ we have: $M_{-1,CM} = 1/8$, $M_{1,CM} = 1/2$ and $M_{3,CM} = 2$.

While the strength and energy of the c.m. excitation remains constant as a function of g , the energy and strength of the peak due to the intrinsic motion depends on g . In particular the strength is an increasing function of g going from $1/4$ at $g = 0$ to $3/4$ when $g \rightarrow \infty$. This increment of the strength of the intrinsic peak associated to the mono-pole vibration is the main reason for the increasing behaviour of the different sum rules as a function of g . For all values of g , the peaks associated to the C.M. and to the breathing mode exhaust more than the 99 % of the sum rules and the higher peaks have a small but not negligible influence.

It is also illustrative to compare the $g \rightarrow \infty$ value with the Thomas-Fermi one, in this case the kinetic energy is neglected and the estimate of the excitation energy from the sum rules is, $E_{exc} = \sqrt{3}$. Thus, as emphasized in [23], the reentrant behavior is a clear consequence of the "fermionization" taking place as the $g \rightarrow \infty$. In 1D gases with contact interaction increasing the interaction strength, the approximation which is sensible is to neglect the interaction energy keeping the kinetic one, unlike

in the Thomas-Fermi limit where the kinetic energy is neglected in front of the interaction.

7.2 Excitation energy and reentrant behaviour

In the calculation of $S_F(E)$ in a previous chapter, we have observed that the two important peaks (C.M. and breathing mode) of $S_F(E)$ are rather close to each other. Therefore, one expects that the estimation of the breathing excitation energy through the sum rules should be rather accurate. In Fig. 7.2 we compare the mono-polar excitation energies estimated by means of the sum rules described above with the values of the excitation energy of the breathing mode.

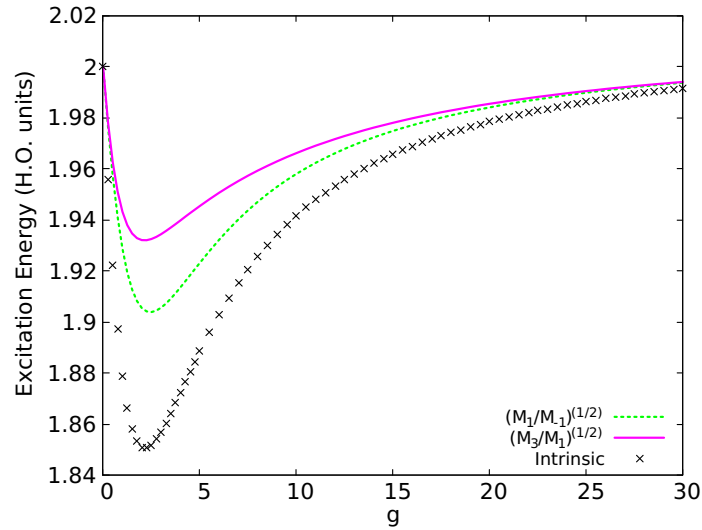


FIGURE 7.2: Mono-polar excitation energy estimated using $E_{ex} = \sqrt{M_3/M_1}$ and $E_{ex} = \sqrt{M_1/M_{-1}}$ compared to the one from the breathing mode itself. In the non-interacting limit and in the Tonks-Girardeau limit they reach the value $E_{ex} = 2$. For $g \approx 2$ we can depict a minimum of E_{ex} leaving us with the reentrant behaviour. The sum rules have been computed using $m=200$ (101 modes).

Notice that in all cases, the estimate $\sqrt{M_3/M_1}$ is larger than $\sqrt{M_1/M_{-1}}$ for any value of g and both are larger or equal than the minimum excitation energy defined by the breathing mode. First we note that the two quantities obtained from $\sqrt{M_3/M_1}$ and $\sqrt{M_1/M_{-1}}$ do not produce the same estimate for the intrinsic mono-polar excitation energy. This reflects the fact that the structure function contains two relevant excited states not located at the same energy, one from the center of mass and the second from the breathing mode. The difference between the two estimates provided by the sum rules increases with g and is larger for the value of g that maximizes the interaction energy. For this value of g the difference in energy between the C.M. excitation and the energy of the breathing mode is also maximal. Then, when g increases further and the breathing mode gets closer again to the C.M. excitation, the

estimates get closer and both reach asymptotically the $E_{ex} = 2$ when $g \rightarrow \infty$.

The reentrant behaviour of the breathing mode previously discussed is clearly reproduced by the estimations of the excitation energies provided by the sum rule analysis. If we subtract the contribution of the C.M. to the sum rules, it is equivalent to study only the intrinsic excitations, see Fig. 7.3. In this case there is only one dominating peak: the breathing mode and consequently, the estimations of the excitation energy from the sum rules are much closer. The differences in this case should be assigned to the higher excitations beyond the breathing mode.

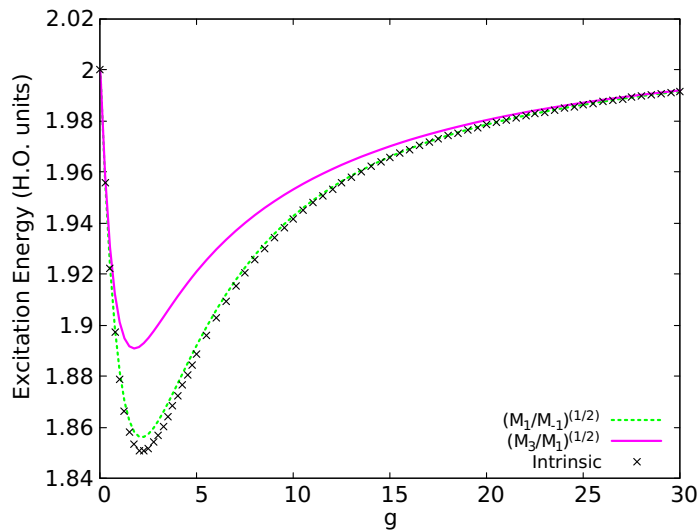


FIGURE 7.3: Intrinsic excitation energy of the breathing mode compared to the mono-polar excitation estimations using $E_{ex} = \sqrt{M_3/M_1}$ and $E_{ex} = \sqrt{M_1/M_{-1}}$, where the C.M. contribution has been extracted. In both limits they all reach the value $E_{ex} = 2$, and there is a minimum that signals the reentrant behaviour around $g \approx 2$. These new estimations are a good approach to the breathing mode excitation energy. The sum rules have been computed using $m=200$ (101 modes).

Chapter 8

Summary and Conclusions

In this thesis we have considered a 1D gas of ultra-cold bosonic atoms, where the atom-atom interaction is assumed to be well represented by a delta contact interaction. This system has already been realized experimentally in two ultra-cold atomic laboratories and is expected to be studied in more detail in future experiments. Our main aim has been to explore the properties of the system, i.e. wave functions, excitations, correlations, etc, as the strength of the atom-atom interaction is varied. The latter is possible in ultra-cold atom experiments by means of Feshbach resonances.

In the first chapter, we considered the homogeneous system. In this case, we introduced already the two noteworthy limiting cases, the zero interaction case, in which the system fully condenses and the infinitely strong interaction case, which gives rise to the Tonks-Girardeau gas. We have shown some of the properties of the TG gas, like the impossibility of finding two particles at the same position, as revealed by pair correlations.

Then we have concentrated in the case of N bosons trapped in a harmonic oscillator potential. In this case, we have first derived a virial relation which holds for both bosons and fermions and which is very useful to cross check numerical calculations. Afterwards we have discussed the two limiting cases, discussing the properties of both the condensate and TG gas. Then we have derived the Gross-Pitaevskii equation, which is obtained in the mean-field approximation. As expected, this description fails to capture the properties of the N -body system when the interactions are not small or for very small number of particles, where more involved quantum correlations appear in the system.

After the general case, we have concentrated in the two-boson case. We have explained in detail the spectral properties of the system as a function of the interaction parameter, discussing also the different contributions of the energy. Notably, the interaction energy provides a good witness of the presence of correlations: for small interaction strength the interaction energy increases with the strength. At sufficiently large interaction strength, the system starts to build quantum correlations to avoid the contact, which in turn result in a decrease of the interaction energy as we further increase the interaction strength.

The study of the spectral properties has been the main objective of the last two chapters. This has been done by computing the dynamic spectral function for a

mono-polar excitation. In particular, we have thus considered the excitation of the breathing mode, i.e. the first excitation of the relative motion of the atoms. This breathing mode had been previously shown to exhibit a reentrant behavior as the interaction strength was varied from 0 to large values. We have demonstrated that this is indeed the case for the two-particle case, and also that other relative excitations exhibit a similar reentrant behavior.

Finally, we have explained how information about the mono-polar excitation can be obtained from ground state properties by means of energy sum rules, which were originally introduced in nuclear physics. We have shown how the squared ratio of two moments of the distribution can be used to obtain estimates for the breathing mode energy. This is the technique used in quantum Monte-Carlo calculations in which only ground state properties can be computed. Our method allows us to explore the quality of this approach for different squared ratios of the sum rules in the whole range of interaction strengths considered.

Bibliography

- [1] Hans-Werner Hammer, A. Nogga, and A. Schwenk, *Rev. Mod. Phys.* **85**, 197 (2013)
- [2] F.E. Close., *An introduction to quarks and partons*, Academic Press (1979)
- [3] F. Serwane, G. Zürn, T. Lompe, T. B. Ottenstein, A. N. Wenz, and S. Jochim, *Science* **332**, 336 (2011).
- [4] G. Zürn, F. Serwane, T. Lompe, A. N. Wenz, M. G. Ries, J. E. Bohn, and S. Jochim, *Phys. Rev. Lett.* **108**, 075303 (2012).
- [5] A. N. Wenz, G. Zürn, S. Murmann, I. Brouzos, T. Lompe, and S. Jochim, *Science* **342**, 457 (2013).
- [6] S. Murmann, A. Bergschneider, V. M. Klinkhamer, G. Zürn, T. Lompe, S. Jochim, *Phys. Rev. Lett.* **114**, 080402 (2015).
- [7] L.P. Kouwenhoven et al., *Rep. Prog. Phys.* **64**, 701 (2001)
- [8] E. Haller, M. Gustavsson, M.J. Mark, J.G. Danzl, R. Hart, G. Pupillo, Hanns-Christoph Nägerl, *Science* **325**, 1224 (2009)
- [9] I. Bloch, J. Dalibard, and W. Zwerger, *Rev. Mod. Phys.* **80**, 885 (2008)
- [10] X. He, P. Xu, J. Wang, and M. Zhan, *Opt. Express* **18**, 13586 (2010).
- [11] R. Bourgain, J. Pellegrino, A. Fuhrmanek, Y. R. P. Sortais, and A. Browaeys, *Phys. Rev. A* **88**, 023428 (2013).
- [12] G. Pagano, M. Mancini, G. Cappellini, P. Lombardi, F. Schäfer, H. Hu, X.-J. Liu, J. Catani, C. Sias, M. Inguscio, and L. Fallani, *Nat. Phys.* **10**, 198 (2014).
- [13] A.M. Kaufman, B.J. Lester, M. Foss-Feig, M.L. Wall, A.M. Rey, C.A. Regal, *Nature* **527**, 208 (2015).
- [14] T. Busch, B-G. Englert, K. Rzazewski, and M. Wilkens, *Found. Phys.* **28**, 549 (1998).
- [15] F. Dalfovo, S. Giorgini, L. Pitaevskii, S. Stringari, *Rev. Mod. Phys.* **71**, 463 (1999).
- [16] E. Braaten, H.W. Hammer, *Physics Reports* **428** (5-6), 259-390 (2006)
- [17] M. Girardeau, *J. Math. Phys.* **1**, 516 (1960)
- [18] E.H. Lieb and W. Liniger, *Phys. Rev.* **130**, 1605 (1963)

- [19] M. A. Cazalilla, R. Citro, T. Giamarchi, E. Orignac, and M. Rigol *Rev. Mod. Phys.* **83**, 1405 (2011)
- [20] V.I. Yukalov and M.D. Girardeau, *Fermi-Bose mapping for one-dimensional Bose gases*, Arxiv Notes (2005)
- [21] A. M. Kaufman, B. J. Lester, C. M. Reynolds, M. L. Wall, M. Foss-Feig, K. R. A. Hazzard, A. M. Rey, C. A. Regal *Science* **345**, 306-309 (2014)
- [22] B. Paredes, A. Widera, V. Murg, O. Mandel, S. Fölling, I. Cirac, G. V. Shlyapnikov, T. W. Hänsch, I. Bloch, *Nature* **429**, 277 (2004).
- [23] A. Iu. Gudyma, G. E. Astrakharchik, Mikhail B. Zvonarev, *Phys. Rev. A* **92**, 021601 (2015).
- [24] R. Schmitz, S. Krönke, L. Cao and P. Schmelcher, *Phys. Rev. A* **88**, 043601 (2013).
- [25] O. Bohigas, A. M. Lane, J. Martorell, *Phys. Rep.* **51**, 267 (1979).
- [26] W. Tschischik, R. Moessner, and M. Haque, *Phys. Rev. A* **88**, 063636 (2013).
- [27] R. J. Swenson, *Physics Letters* **29A**, 693 (1969)
- [28] S. Stringari, *Phys. Rev. Lett.* **77**, 2360 (1996).
- [29] D. L. Bartley, V. K. Wong, *Phys. Rev. B* **12**, 3775 (1975)
- [30] V. Dunjko, V. Lorent, M. Olshanii, *Phys. Rev. Lett.* **86**, 5413 (2001)
- [31] T. Kinoshita, T. Wenger, D. S. Weiss, *Science* **305**, 1125 (2004).
- [32] F. Deuretzbacher, K. Bongs, K. Sengstock, D. Pfannkuche, *Phys. Rev. A* **75**, 013614 (2007).
- [33] P. Mujal, E. Sarlé, A. Polls, B. Juliá-Díaz, *Phys. Rev. A* **96**, 043614 (2017).
- [34] M. Andrii Gudyma dissertation, *Non-equilibrium dynamics of a trapped one-dimensional Bose gas*, Université Paris-Saclay
- [35] Frank Deuretzbacher dissertation, *Spinor Tonks-Girardeau gases and ultracold molecules*, Universität Hamburg (2008)
- [36] P. Ring, P. Schuck, *The Nuclear Many-Body Problem*, Springer-Verlag
- [37] P. Kosciuk, T. Sowinski, *Exactly solvable model of two trapped quantum particles interacting via finite-range soft-core interactions*, Arxiv Notes (2018)

